1 Basic principles and concepts

> Thoughts without content are empty, intuitions without concepts are blind.
> Immanual Kant, Critique of Pure Reason, B25, 1781.

1.1 Introduction

Foams can exist in the wet, dry or solid state and can be seen almost everywhere, in the home, in the surrounding natural environment and in numerous technological applications. In fact they are prevalent, and it is almost impossible to pass through an entire day without having contact with some type of liquid or solid foam. They have several interesting properties which enable them to fill an extremely wide range of uses; for example, they possess important mechanical, rheological and frictional characteristics which enable them to behave similar to solids, liquids or gases. Under low shear, wet (bubbly) foams exhibit elastic properties similar to solid bodies, but at high shear, they flow and deform in a similar manner to liquids. On the application of pressure or temperature to wet foams, the volume changes proportionately, and this behavior resembles that of gases. Interestingly, it is the elastic and frictional properties of wet foams which lead to their application in personal hygiene products such as body lotions, foaming creams and shaving foams. While shaving, foam is applied to the skin and the layer on the blade travels smoothly over the surface, reducing the possibilities of nicking and scratching. Another example is their use as firefighting foams, where properties such as low density, reasonably good mechanical resistance and heat stability are required in order to be effective in extinguishing gasoline fires. Essentially, they act by covering the flames with a thick semi-rigid foam blanket. The low density allows the water in the foam to float even though it is generally denser than the burning oils. The chemical composition and mechanical properties of these types of foams can be varied to optimize the firefighting utility.

Foams are also found in many food items, either in finished products or incorporated during some stage in food processing. They primarily provide texture to cappuccino, bread, whipped cream, ice-cream topping, bread, cakes, aerated desserts, etc. Surprisingly, several novel types of food foams have been recently produced from cod, mushroom and potatoes, using specially designed whipping siphons powered by pressurized gas with lecithin or gelatin as alternative foaming agents to replace egg and

creams (1). Several modern architectural designs and works of art have also been manufactured from bubbles and foams, and they are also used for entertainment purposes. Foam and bubble exhibitions frequently take place at the Science Museum, London, where young children are enclosed within soap bubbles and foams. In fact, it has been reported that 50 children were packed inside a soap bubble which became a world record (2). Foams play an important role in evolution, particularly in the insect and animal world. For example, while female frogs lay eggs they also secrete a fluid which is whipped up into foam by the male frogs, and this robust foam protects the eggs by becoming a shield against the physical and biological environment.

Foaming also occurs in cleaning and detergency which is utilized in cleaning factories, shops, offices, machines, factories, cars, workshops, garages, floors, etc. In many of these applications, it is important to optimize the extent of foaming. This has been achieved by manufacturers synthesizing new types of low-foaming nonionic chemical detergents. However, in some applications where customers prefer to see some foam, small amounts of special foam-producing substances were included in their product as foam improvers, boosters or foam stabilizers. During the 1950s and 1960s, wet detergent-based foams were well known to cause major problems when discharged into streams and rivers. They were often odorous, and when rivers flowed over weirs, the foams frequently increased in height and were frequently blown into neighboring environment. However, over the past 50 years, more effective biodegradable (green) surfactants (soft detergents) have been developed which considerably reduced foaming.

Often wet (bubbly) foams have been formulated to perform specific functions such as decontamination control (e.g. for cleaning materials inside nuclear reactors) and in oil-recovery, agriculture and beverages such as Guinness stout, where the foam head must remain stable during pouring and consumption. In addition, the method of generating foam is dependent on the application and requirements of the foam. In Fig. 1.1, four different everyday foams are shown. While firefighting and shaving cream foams are produced by release of gas under pressure, the bubbles in Guinness foams are produced by fermentation, and detergent foams are produced by entrapment of air during agitation.

In most cleaning operations, the foaming performance is not necessarily related to the volume of the foam or stability, although different applications may require different amounts of foam with an abundance of foam usually preferred in body-cleaning products. However, this is not the situation for washing machines where vigorous agitation occurs and foam volume needs to be minimized. Foams can often cause problems in commercial processes such as in paper-making and distillation where over-production of wet foams leads to loss of efficiency and downtime in plant production. Under these circumstances, it is often necessary to add antifoamer, defoamer or foam breakers (3).

Foams are also capable of immobilizing large volumes of air and combining lightness in weight with strength and elasticity, and these properties are critical in their use in many well-established industrial processes such as froth or foam flotation. This is one of the largest and most important industrial uses of bubbles and wet foams which have been

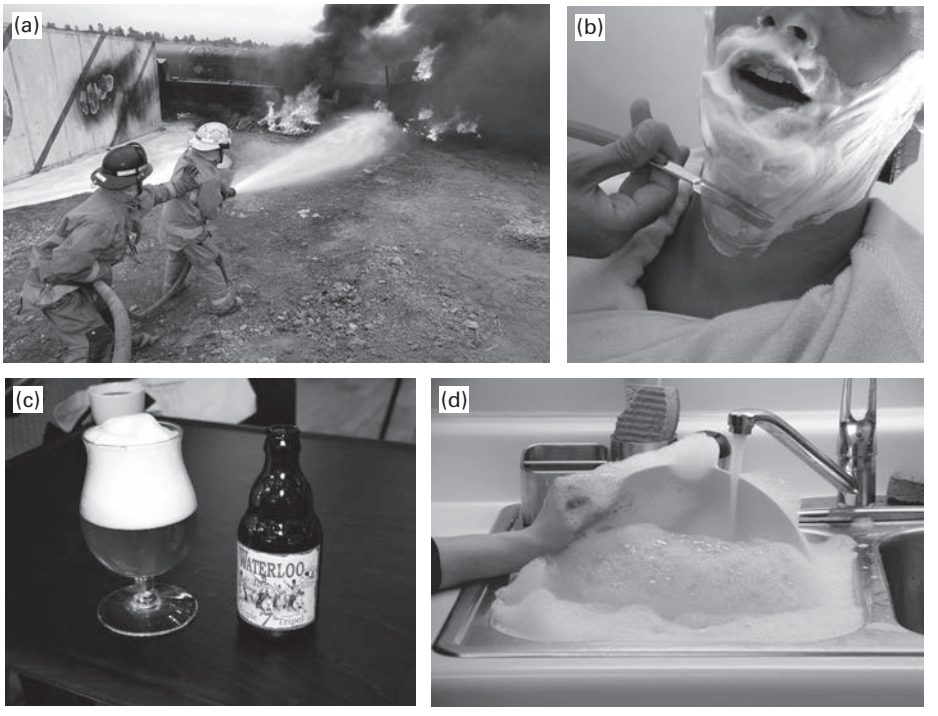

Fig. 1.1 Applications of wet foams. (a) Firefighting foams act to cover or blanket out the flames (prevent air reaching the fire) and must remain stable at high temperatures. (b) Shaving foams are designed to give rheological flow properties (similar to an elastic solid). (c) Beer foams such as Guinness are stabilized by a protective film of proteins which define the texture and enhance the flavor and retain their stability until the beer is consumed. (d) Detergent foams (in dishwashing) are stabilized by low molecular weight synthetic surfactants.

used for more than 100 years. During the extraction of mineral ore, it is necessary to separate the particles by flotation so that the more valuable hydrophobic ore particles (sulfides of copper, zinc, gold, etc.) adsorb at the foam interface and remain suspended by capillary forces while the less valuable hydrophilic particles (usually silicates) sink in the liquid (4). The amount of ore that can be separated for a given amount of liquid is directly proportionate to the surface area of the foam (bubbles), and huge masses of ore can be easily processed using relatively small volumes of water. Figure 1.2(a) shows a schematic drawing of a foam or froth flotation cell, and Fig. 1.2(b) shows a typical foam of froth.

The terms "foams" and "froths" which can be considered as weakly stabilized foams are often used interchangeably, but in industry a three-phase system (a gas–water macrocluster with dispersed particles) is considered a froth, and a structure containing only the gas and liquid phases is considered a foam. The link between the stability of a flotation froth and flotation performance has been investigated both in the plant and in the laboratory by using a modified a froth stability test column (5). In this test, a gas is continuously sparged into a foaming solution, and simultaneously froth collapses at its free surface occurs. When the rate of froth collapse equals

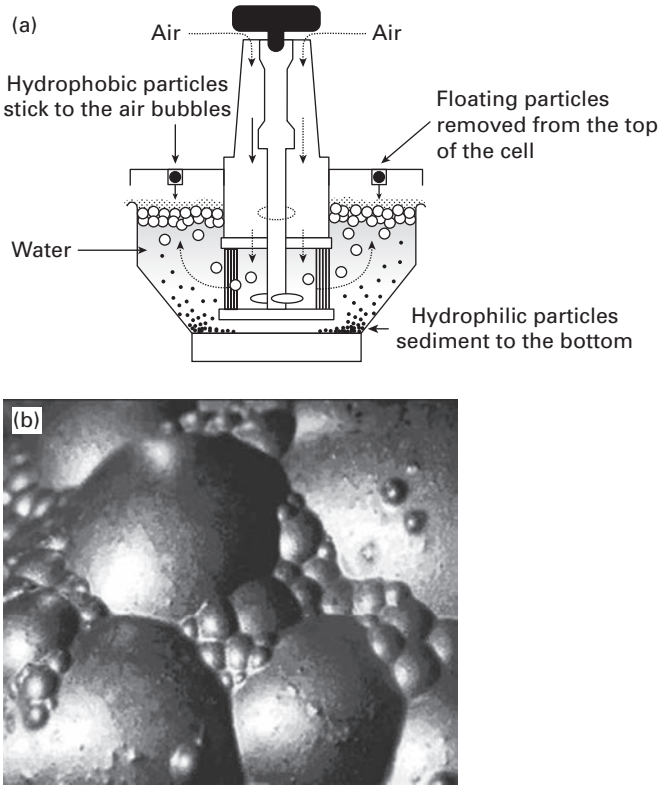

Fig. 1.2 (a) Schematic representation of a flotation cell and (b) the froth of foam with particles attached to the bubbles. Flotation of mineral particles is the largest industrial application of bubbles and foams. The process involves the separation of the more valuable minerals such as copper, zinc and lead from the less valuable silicates. Billions of tons of ore are treated annually using this technology.

the rate of generation of fresh froth, an equilibrium height is attained. The equilibrium foam height, divided by the superficial gas velocity, is used as a measure of froth stability. From these studies, it was found that the variations in flotation performance are directly related to changes in froth stability. In addition to mineral processing, froth flotation has also been successfully used in other separation processes such as the treatment and recycling of effluent, proteins, plastic wastes, etc. The flotation process is also extremely important in the deinking of waste paper (6) and enabling recycling of about 30% of paper. Foams also play an important role in the extraction of residual oil from porous rocks (7).

Although this text is mostly limited to wet foams, it is also important to note that solid polymeric foams (which are usually oil based and are usually manufactured from wet foams) are generally considered as a specific group of material foams. They can be classified as rigid, semi-rigid, semi-flexible or flexible depending on cellular morphology, composition and other physical characteristics. They are manufactured with a specific range of properties, achieved by controlling the degree of crystallinity

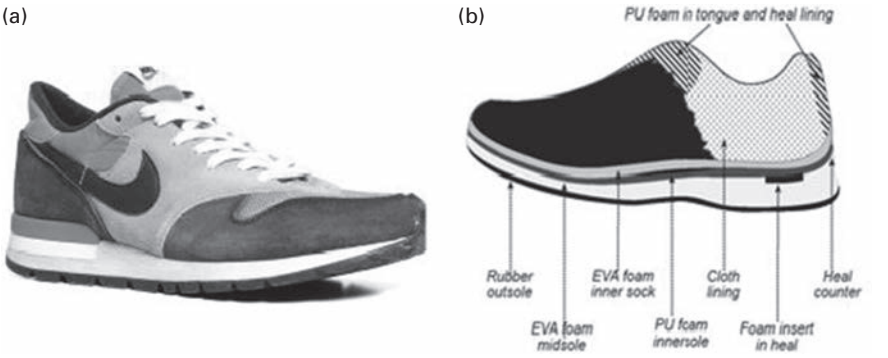

Fig. 1.3 Running shoe showing some of the important foam polymers which are used as components.

and the extent of cross-linking of the polymeric framework. Close-cell material foams contain cells that are permanently trapped (isolated). In other cases where the cells are open or connected to neighboring bubbles by gas channels, both gas and solid may be considered to exist as continuous phases. However, only closed-packed structures are regarded as true polymer foams, and these products are more expensive to manufacture therefore, the cells are filled with special gases to improve insulation. Self-skin foams are frequently found, for example, in shoe soles and mattresses and are often manufactured with high-density skins and low-density cores. Open cells have networks or channels which allow air to flow (e.g. polyurethane seat cushion).

Their properties are extremely dependent on the method of preparation and manufacturing particularly during the solidification. Most close-cell foams have fairly rigid structures, but open-cell foams have been developed which are generally more flexible. Originally, foamed rubber and phenol-formaldehyde and urea-formaldehyde resin foams were developed in the early 20th century followed by more specific foam polymers such as polyurethane (PU), polystyrene (PS), ethylene-vinyl acetate (EVA) and polyvinyl chloride (PVC). Many specialized polymer foams have been developed for the consumer market, and these have been utilized in numerous applications in recent years. For example, a considerable amount of research and development has been invested in foams for lightweight running shoes where low mass is needed to reduce the energy consumption of the athlete. Figure 1.3 shows the cross-section of a pair of trainers, indicating the different sections and major foam components.

Several foam component parts such as the rubber innersole and the foam midsole compression which is molded from EVA copolymer are used to provide cushioning or control torsion of the foot. The foams have been developed to withstand compression and bending loads caused by feet. PU foams have been used as an alternative to EVA for midsoles, but the density of PU is higher although the compression is lower. The shoe components are bonded together so that adhesive action of the foam is important. Different gases are often used in these types of foams. For example, Nike's large bubbles contain SF_6 gas as an insert in the main foam. Another recent development is the memory foam footbed. Most major shoe manufacturers show their design innovations on websites. A background on the polymer/structural properties relationships is given

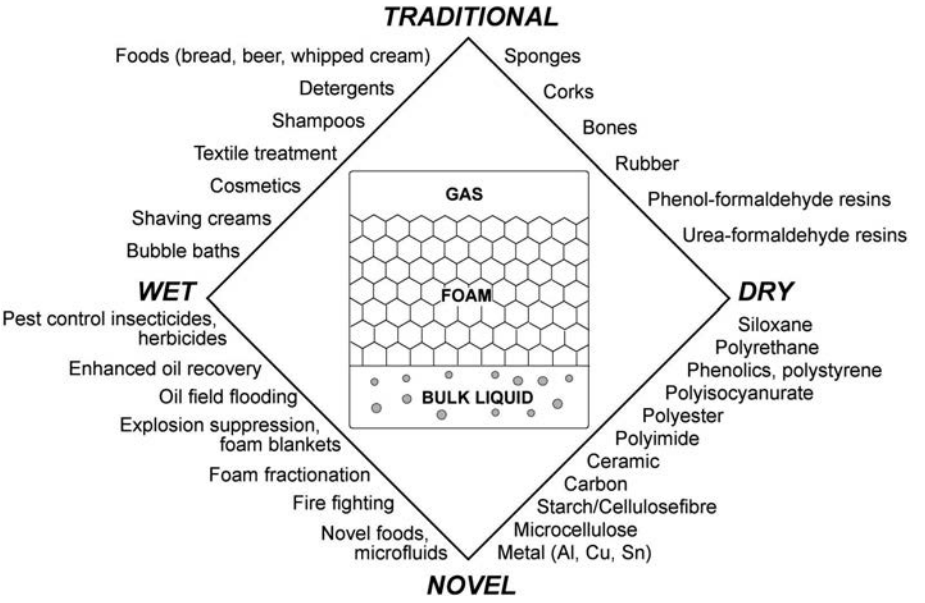

Fig. 1.4 In the figure, along the lower right side, Cellulose fibre Important traditional and novel applications of wet and dry foams.

by Mills 2005 (8), while information on the application of foams has been published on several websites (see, e.g., www.foamstudies.bham.ac.uk).

Polymer foams are also widely used in boats, aircraft furnishing, cycle helmets, etc. and are manufactured from a variety of plastics and polymers. They are also used as light-weight cellular engineering materials which require a high strength to weight ratio, for space applications and have been used as core material in sandwich-structured composites. The combination of low weight and unique elastic properties are ideal for packing and cushioning, and polyurethane is used in the manufacture of seat covers and chairs whereas foamed polystyrene is used as take-out boxes, trays in restaurants, coffee cups in cafes, seat cushions, car seats, car bumpers and thermal or sound insulations. In addition to polymers, rigid dry foams may be produced from metal, glass, concrete and ceramics, and these have found widespread application in, for example, domestic insulators, air conditioners and reinforcements. They are used for thermal insulating, vibration damping and for acoustic absorption. Following the introduction of material foams, the principles governing the more advanced technology has become fairly well established, and it has become possible to match the effective properties such as stiffness or rigidity, strength, compression to the cellular architecture. Overall, both wet and dry foams cover a wide range of both traditional and novel applications, and many of these have been summarized in Fig. 1.4.

Novel and potential application of foams are frequently reported in the daily press. For example, an expanding foam has recently been developed that could be pumped into bodies of wounded soldiers to reduce internal bleeding (9). The technique involves injecting two chemicals into the badly injured soldier's abdomen which react to generate a rapidly expanding foam which solidifies and seals the injuries in the body organs,

preventing the loss of blood. This gives sufficient time for the soldier to be taken to a field hospital where the foam can be easily removed by surgeons. It is also shown as a potential bone substitute. Bone has a compact surface with a cellular core and is composed of both mineral substances and tissues. The bone tissues are made up from cells, fat and natural polymers (such as polysaccharides, collagen, polyphosphates, etc.). Recent developments in synthetic foam technology have led to the production of cellular materials from starch-based (biodegradable) polymers and polyethylene (bio-inert) polymers as possible replacements for bones (10). Syntactic dry foams have also been developed containing hollow particles such as glass ceramic and polymer spheres embedded in a matrix material. In the literature, numerous separate texts have been published covering specific types of polymer foams – for example, polyurethane or polystyrene foams.

1.2 The physics and chemistry of foams and foaming

Although foams have been shown to be extremely useful from the industrial viewpoint, they have, in addition, unique academic appeal within the physical chemistry, physics and biophysics communities from a scientific viewpoint and have served as useful models for numerous investigations over several centuries. Foams have been studied extensively within both universities and industrial laboratories. Foams are extremely complex systems, and early fundamental studies by Thomas (11) showed a basic relationship between soap foams and the cellular structures of plants and animals. This approach has led to a deeper understanding of natural processes through which many biological systems emerge. Also similar structural features have been revealed during grain growth in metallurgical systems (12). Within the physics community, a strong emphasis has been placed on the mechanics, film permeability, rheological properties (such as the variation in elasticity with gas fraction) and the structural rearrangements occurring as the bubbles become less spherical and more highly packed during the transition from wet to dry foam. In fact, it is the liquid content and geometry (surface area, bubble size and size distribution, shape (compaction) and order/disorder which are considered to be important parameters to consider, since these can lead to a fundamental understanding into the relationship between the scaling and structure. Most of the pre-1999 studies dealing with basic static and quasi-static properties of dry foams have been well described in the classic book by Weaire and Hutzler, entitled *The Physics of Foams* (13). More recently, Drenckhan and Saint-Jalmes presented a historical perspective entitled *The Science of Foaming* from a physicist viewpoint (14).

Physicists and mathematicians have been contemplating the structure of foams over a considerable period of time, often focusing on idealized ordered foams. However, ordered foams are not very diverse and collectively contain only a few kinds of cells, whereas real foams are disordered and contain a variety of shapes. Many theoretical computer simulations have been carried out over the past 20 years, using the Surface Evolver (15) to compute the evolution and equilibrium structures of foams, and this has

been found to enhance the understanding of real foams physics. The Surface Evolver is an interaction program which can be used to derive a minimal energy surface or to model the process of evolution of a surface which is shaped by surface tension and other energies such as gravitational energy, squared mean curvature, etc. The program evolves the surface toward minimal energy by a gradient descent method. It is also necessary to introduce user-defined surface integrals or knot energies. For example, computations on the equilibrium microstructure of soap films with random structure and with a wide range of cell-sized distributions have been reported (16).

For many experimental foam studies, physicists need a convenient highly reproducible sample which was assumed to be stable for extended time periods. Plateau (17) used a soap solution to produce thin films and foams but had difficulties in achieving sufficient stability. Later, formulations were improved by the addition of glycerin which raised the viscosity and retarded the evaporation of water, and since then many different types of chemical recipes have been described which produce highly stable foams. Strong (18) has published a long list of formulations for preparing foams with extremely long lifetimes. Over the past 50 years, numerous experimental studies have been carried out by physicists based on a stable foam system: a commercial shaving cream (Gillette foam regular) is produced by an aerosol method. This is a complex mixture, comprised of an aqueous solution of mixed ionic surfactants (triethanolamine and stearic acid) which is supersaturated with hydrocarbon gases. On release of the contents, the bubbles are generated from solution with the surfactants adsorbing at the bubble interface which stabilizes the foam. This system produces nearly spherical bubbles (with 20–30-micron diameter and a gas fraction of about 0.92) which are highly stable for more than 24 hours with negligible drainage within this period due to the high viscosity. More recently, the physics community has shifted toward the dynamic rather than the static nature of wet foams, and many studies have been documented which involve the creation and manipulation of relatively small, discrete and equal volume-sized bubbles which have a tendency to self-order under confinement while producing crystalline and microfluidic foam structures (19). Such monodispersed foam systems have been shown to have many useful applications in areas such as templating, colloids and granular systems.

However, for the physical chemist most of the attention has been focused on the mechanisms involved in stabilization and destabilization and the surface-active materials (which may be chemicals, polymers, particles or mixtures) in wet foams and their role in their assembly in the interfacial layers. Numerous papers and several books have been published on foam generation, stabilization, antifoaming/defoaming and foam films (20). It has been shown that the both dynamic and equilibrium surface tension and interfacial rheology play important roles in defining the foaming characteristics and overall structure of the foam. Wet foams are, in reality, stabilized by a huge range of different types of surface-active agents that adsorb at the interface and reduce the free energy or tension. Hence, from the chemical aspects, it is the adsorption kinetics and type and amount of surface-active agent at the gas and liquid interfacial which play an intricate role in the generation of foam. Collapse and instability usually involves film

rupture and frequently depends on the sensitivity of the chemical composition and structure of the adsorbed film. Stability is more dependent on the viscoelasticity properties and the repulsive interaction between the film lamellae. In fact, changing the concentration of the surfactant or the introduction of alternative surfactants (antifoamers or foam boosters) or mixtures enhances or reduces the generation and stability of the foam.

1.3 The wetness and dryness of foams

Foam properties depend on the gas fraction in cases where they contain low volumes of gas, and the bubbles that are spherical are usually referred to as bubbly liquids or bubbly foams. At high gas content, they are no longer spherical and thus behave as solids with a high shear modulus. Under these circumstances, elastic energy is required to shear the network. In his classic text in 1973, Bikermann (21) defined wet foams as systems where the volume of gas is much lower so that they can be called an agglomeration of gas bubbles, and this state occurs where the bubbles are separated from each other by thin liquid films. Each bubble is so closed that it has no gas-filled channels which can connect between neighboring bubbles. However, more generally, the system could be wet or dry, and in cases where a connection exists and there is a continuous gas phase, it is considered as an open foam structure. Cork, wood, coral and sponges are dry natural foams, whereas with bread (a man-made foam) the yeast produces small bubbles which grow into a close-cell structure (Fig. 1.5). However, if the bread is allowed to rise excessively, it develops into a dry open-cell structure with the spaces interconnected by threads of paste. Generally, a rigid dry foam system is usually regarded as a special class of dry foam produced by an irreversible chemical process.

The evolution toward dry foam proceeds by the reduction of water from the system, and it is usually caused by liquid drainage under gravity and by the suction produced by the pressure gradients that exist between regions of different curvature (capillary suction). Overall, wet foams may essentially be regarded as naturally evolving non-equilibrium systems, consisting of a collection of coarse polydispersed gas bubbles, packed into a smaller volume of liquid. In the case of pure water, the bubbles usually burst but in the presence of a sufficiently high enough concentration of surfactant, the liquid drains away gradually and the curved bubble surfaces are gradually transformed into characteristic irregular polyhedral foam cells bounded by thin soap films with almost plain surfaces of contact. The transitions in structure which occur from wet to dry foam systems are illustrated by the two-dimensional (2D) scheme in Fig. 1.6.

Generally, the liquid fraction of a foam is defined by the ratio of the volume of liquid to the total volume of the foam. Aqueous foams typically contain as much as 95% gas and 5% liquid, with the aqueous phase consisting of 99% liquid while the remaining 1% is the vital surface-active ingredients (typically a chemical surfactant). In general, the structure and dynamics of foams are determined by the amount of gas in the system, and the ratio of gas to liquid is defined as the foam number or wetness. However, the liquid

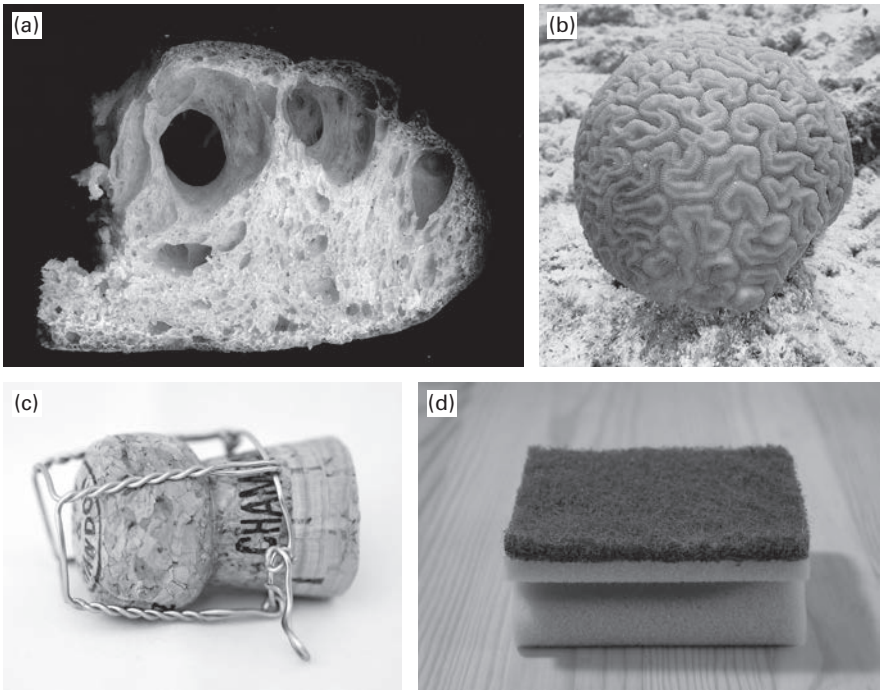

Fig. 1.5 Common types of dry foams. Bread exhibits a close-cell structure, but coral, cork and synthetic sponges show open-cell structures.

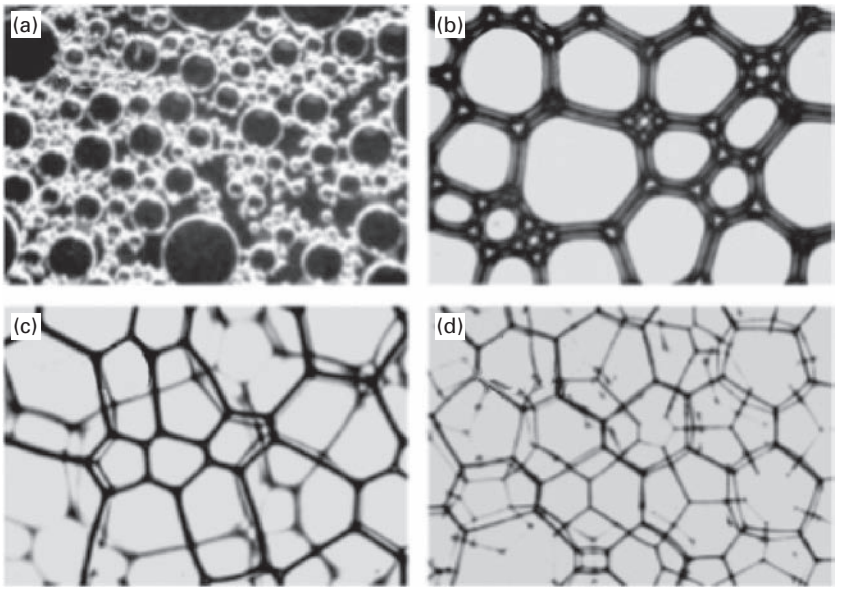

Fig. 1.6 Schematic 2D representation of a wet and dry foam with different volume fractions. (a) Very wet non-drained foam consisting of non-interacting bubbles; (b) wet foam partially drained with interacting bubbles causing deformation; and (c) further drainage causes lamellae to further thin and swell in the Plateau borders. (d) Finally, a well-drained foam. Dry foam consisting mostly of gas phase entrapped in polyhedral cells separated by thin films with thickness <100 nm. Note curvature of some bubbles walls owing to unequal internal pressures. The nature of the thin film has been subject to intense study. From ref (22).

fraction may vary from about 1% (which is considered a dry foam by the physics community) to about 35% (a wet foam). During the transformation from spherical (polyederschaum) to polyhedral structure, the water content or degree of wetness of the foam changes (as expressed by its liquid volume fraction Φ_l or gas volume fraction Φ_g). These two values are interrelated, as seen from the equation

$$\Phi_l = 1 - \Phi_g \tag{1.1}$$

The critical gas fraction $\Phi_{g,critical}$ is defined as the value of Φ_g in which the individual bubbles are spherical, and this state is most commonly considered as a bubbly liquid. Higher values of Φ_g cause deformation of the bubbles. In order to obtain a gas fraction of $\Phi_g > \Phi_{g,critical}$ a force is required to drive out the liquid from the foam. For a typical foam with polydispersed gas bubbles, the value of $\Phi_{g,critical}$ is about 0.72. As Φ_g approaches unity then the foam takes on a polyhedral structure, and calculations give a value $\Phi_{g,critical} = \pi(2\sqrt{3})^{-1} \cong 0.907$ for a 2D model of a mondispersed (hexagonal) foam. For a polydispersed (disordered) foam, $\Phi_{g,critical}$ has a value of 0.84 from a computer simulation (13); Φ is sometimes called the wetness and the ratio of foam volume to the volume of liquid in the foam; and $(1/\Phi)$ is the expansion factor or expansion ratio. The relative density is the ratio of the density of wet and dry foams, and defined as $\rho_R = \rho_f/\rho_l$ and for polymer foams $\rho_{RP} = \rho_f/\rho_e$, provided there is no filler or solid additives.

1.4 Capillary pressure and the Laplace–Young equation

One of the most important relationships which define the transitional states in wet and dry foam structures is the balance between the capillary pressure within the thin foam films and the drainage of liquid from the structure by gravitational forces. For a gas bubbles (with radius r) submerged in a liquid (in an equilibrium state and in the absence of gravitation forces), the shape must be spherical in order to balance the minimum surface area requirements, and there must be a pressure difference across it. The equation which defines the capillary pressure (or the value of the pressure difference) to the curvature of the surface was deduced independently in the 18th century by Young (23) and Laplace (24). This situation for a bubble is illustrated in Fig. 1.7.

The derivation is as follows: if we take γ is the surface tension of the interface then the total surface free energy of the bubble is $4\pi r^2\gamma$, and if the radius was to decrease by dr then the change in surface free energy would be $8\pi r\gamma/dr$. Since the shrinking in size causes a decrease in the surface energy, then the tendency to do so must be balanced by a pressure difference across the film ΔP (between the inside relative to outside). The work done to achieve this against this pressure difference is $\Delta P 4\pi r^2 dr$ which is equal to the decrease in surface free energy. The relationship between the pressure and surface tension is, therefore,

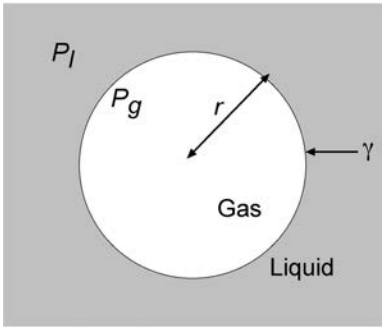

Fig. 1.7 Under equilibrium conditions, the pressure difference (ΔP) between the external pressure P_l exerted from the liquid phase on a gas bubble and the internal gas pressure P_g are related to the radius of the bubble (r) and the surface tension of the liquid (γ) by the Laplace–Young equation.

$$\Delta P 4\pi r^2 dr = 8\pi r^2 dr \quad \text{or} \quad \Delta P = \frac{2\gamma}{r} \tag{1.2}$$

where ΔP represents the pressure difference between the inside and outside of the bubble or the pressure over a curved surface. This pressure is defined as the capillary pressure P_c and is inversely proportional to the radius of curvature and directly proportional to the surface tension. It may be also concluded from Equation 1.2 that for small bubbles, the pressure inside the bubble is greater than that outside. For the general case of soap films, it is necessary to invoke two principal radii of curvature to describe a curved surface so that for bubbles with surfaces of curvature r_1 and r_2 the pressure difference will be

$$\Delta P = \gamma\left(\frac{1}{r_1} + \frac{1}{r_2}\right) \tag{1.3}$$

It may be noted that r_1 is positive if the center of curvature of r_2 lies in the gas phase and also for r_2. However, soap film may be a saddle shape, and in this case the radii must have an opposite sign. Also, in the specific case of $r_1 = -r_2$, the pressure difference ΔP is zero, and this is the situation for a soap film with two plane surfaces. In foam thin film structures, the pressure is lower and the film is thicker in the Plateau border due to the interfacial curvature, so that a capillary suction effect occurs on the liquid from the center of the film to its periphery.

1.5 Plateau rules and pentagonal dodecahedral structures

Foams or froth consist of a random agglomerate of roughly spherical bubbles, and a series of pronounced structural changes occur during draining which eventually leads to the formation of cells. The mean curvature and cell size are important since they affect the gas diffusivity in close-cell foams and the gas flow resistance in open-cell foams. Structural transformation process was originally studied by Joseph

Plateau (Plateau rules) in the 18th century in a series of experiments using soap films constructed on wire frames from which a series of classical geometric rules were formulated. These rules are based on the balance between the interfacial surface tension forces and the surface area of the system which are required to be minimized to ensure the lowering of the Gibbs free energy and stability. The first rule states that when three smooth liquid lamellae are joined by intersecting at every edge, the intersection – formed by any three bubbles (faces) – must come into contact at a point. Once they are stabilized, each pair of intersections form borders with an angle of inclination of exactly 120°. These borders are defined as the Plateau–Gibbs borders and constitute the structural skeleton of the foam (Fig. 1.8). The Plateau borders or edges always number exactly 4, and they meet at a common vertex where the angle is always that of a tetrahedral with the value of 109° and 28 min.

As a bubbly foam drains and the liquid content is reduced, the bubbles gradually transform into an almost regular ideal polyhedrals and from purely theoretical geometric considerations, the regular pentagonal dodecahedron is the ideal lattice shape which almost satisfies the geometric rules. Such a crystal has 12 identical faces, each of a regular pentagon. However, the precise shape of the polyhedral is an unsolved mathematical problem since this structure does not exactly fit or represent an agglomeration of dodecahedrons because the cells cannot completely fill the space without allowing for voids or pores. This situation was initially investigated by Kelvin (25) in 1887 who found that the closest polyhedral structural element which nearly satisfies all the mechanical constraints was a space structure (a filling arrangement) closely resembling the tetrakaidecahedron but with curved edges and non-planar hexagonal faces). From modeling and simulations, a modified version of Kelvin's arrangement of the tetrakaidecahedron, was derived (26). This non-regular polyhedron is known as the β-tetrakaidecahedron and represents an idealized foam structure consisting of a collection of regular tetrakaidecahedron bubbles, with thin films defining the walls and the network unit composed of one node and four liquid-filled half-channels. As the amount of liquid in the channels and modes increases, the mean curvature decreases, and the edges and corners of the polygonal bubbles become more curved. Figure 1.8 shows the structural arrangements of the foam.

Almost 100 years after Kelvin, Weaire and Phelan (27) of Trinity College, Dublin, proposed an improved or counter-solution of Lord Kelvin's conjecture which was derived from a clathrate structure (Na_8 Si_{46}) and was based on two polyhedrons, one with 14 sides and one with 12 sides that nest together in a group of eight, as shown in Fig. 1.9. Their computations show that it has about 0.3% less surface area than Kelvin's solution, and the Weaire–Phelan (WP) structure is at present the lowest energy structure known for an ideal monodispersed foam in dry limit. A giant version of this monodispersed foam structure (consisting of 4500 bubbles) was developed in the architecture design of the Aquatic Centre of the 2008 Beijing Olympics (28).

Interestingly, the WP structure has been recently produced in the laboratory using a container designed so that the walls acted as a template, which was used to capture the

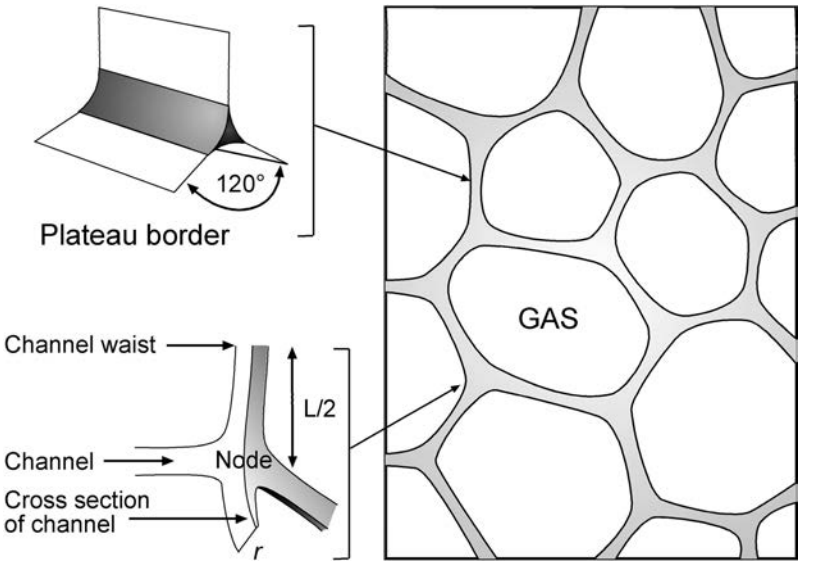

Fig. 1.8 For low liquid fractions almost all the liquid is in the network of Plateau borders. In an idealized foam, four borders join in a tetrahedral arrangement with angles approximately 109°. The liquid network unit is composed of a node and four half-channels. The edge length of the node in each cell is L.

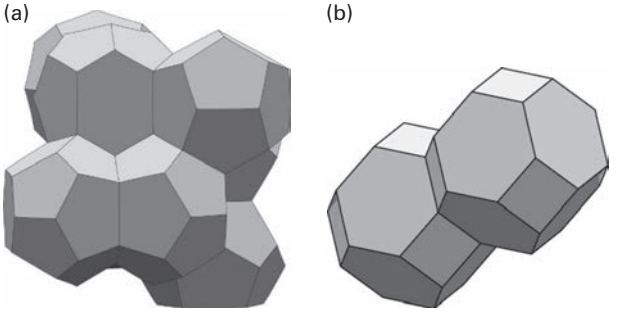

Fig. 1.9 (a) The β-tetrakaidecahedron or modified Kelvin cell. According to Plateau rules, an ideal polyhedral aqueous foam requires the packing of 3D space with repetitions of a polyhedron. A pentagonal dodecahedron is the nearest among regular polyhedrons, but this is not ideal and thus cannot fill space without voids (the packing leaves interstices, and the individual films in a real polyhedral foam are not five sided). A better choice is an irregular polyhedron – the β-tetrakaidecahedron with eight hexagonal and four quadrilateral, with slightly curved surfaces. (b) The Weaire Phelan structure built from a unit cell of six 14-hedra and two 12-hedra.

geometry of the structure. The template was positioned in a surfactant solution and monodispersed bubbles were released from below the template, with the diameter of the bubbles chosen to match the scale of the template (29). The structure was realized on the inner surface of the template walls and corresponded to the 100 faceted planes of the WP structure. In Fig. 1.10, the computer-generated WP structure and the template realization are illustrated. Layers of six bubbles could be formed and the container sealed so that the confined sample contains defect-free monocrystals of the WP structure.

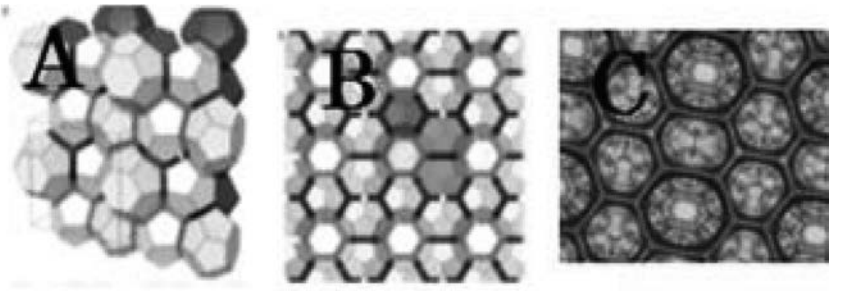

Fig. 1.10 (a) Computer-generated exploded views of two layers of bubbles in the WP structure. Bubble centers in each layer lie on two parallel 100-faceted planes. (b) Frontal view, with the A_3B periodic unit shown. (c) Realization of the WP structure in a pattern mold. From ref (29).

Williams (30) also proposed a modified version of the tetrakaidecahedron structure which consist of two square faces, eight pentagonal faces and four hexagonal faces. This structure had a statistical distribution of face shapes which closely approximates the range of film shapes found in nature, but this has been less used. However, generally, none of these models realistically describes or matches geometric properties of practical foam systems. In the real world, no foam consists of exactly identically sized bubbles, and not all the films between bubbles are planar. There have been various explanations for this non-ideal behavior; for example, Adamson and Guest (31) suggested a simple idea that it may be due to local variations in pressure in the liquid inside the laminas. Such pressure variations would affect the structure and nature of foam drainage.

To summarize, there is no simple model structure that can serve as a convenient mathematic idealization of a polyhedral foam, and real foams are polydispersed and rarely in the shape of Kelvin tetrakaidecahedron. This has been well recognized for a considerable period of time, and early experimental studies by Matzke (32) showed that films consisting of individual bubbles tended to be irregular. From observations of several hundred carefully prepared internal bubbles, it was found that only slightly more than half of the faces were five-sided, and about 10% of the polyhedral structures were pentagonal dodecahedrons. Clearly, pentagons alone cannot completely fill space, but they can be frequently seen within a 3D froth of bubbles such as in detergent solutions. Pentagons are also found in nature – for example, in sea urchin skeletons, turtle shells, insect wings, honeycombs, human fat cells, vegetable cells or metal crystallites. For many years, soap froths were intensively studied since their structures are the archetype for numerous other cellular and biological systems. In fact, it has often been suggested that pentagon symmetry may be related to the five-fold structures often seen in life; for example, five fingers and five toes. All these systems comply with the balance of local forces which constrain to a minimum surface area, resulting in an abundance of pentagonal faces.

Modeling and computer simulations have been used to describe growth and the interaction of soap bubbles in such closely packed formulations. These have proved

useful in solving many difficult geometric problems which frequently involve some form of optimization. Essentially, the topology of the interconnecting of polygons is based on the minimizing of the energy (surface area). This has proved directly applicable to many complex problems such as finding the surface of minimal area between fixed boundaries. For example, calculating the shortest road network between several different cities often needs to be resolved. This also has direct applications to construction and architecture where, again, optimization of resources and materials plays an important role. Within the physics/bubble/foam community, modeling has proved to be extremely useful, and it enables the relationships between liquid content, bubble size and film thickness of foams to be determined. In addition, with dry polymer foams, modeling is frequently applied to predict physical properties such as elasticity and strength.

1.6 Foam structures produced from bubbles with narrow size distributions

The simplest method of generating foams is by shaking together a gas and liquid containing a foaming agent such as a fatty acid soap. Adsorption of the foaming agent occurs rapidly at the gas/liquid interface, causing encapsulation of the bubble and producing some degree of elasticity, which stabilizes the protecting thin film. Due to differences in density between gas and liquid phases, the bubbles (which usually range in size from about 10 microns to 1 cm) float on the surface, generating foam. However, to achieve a 2D bubble or foam raft, it is important to produce bubbles with a narrow size distribution, and this can be achieved in the laboratory by releasing compressed gas at constant gas pressure down a narrow capillary or nozzle (usually about 0.2 to 1 mm diameter) that is immersed in aqueous solution containing foaming surfactant. As the bubble grows, the air/liquid interface expands and floats to the surface, giving an arrangement of different configurations depending on the number of bubbles and their packing configuration at the interface, as shown in Fig. 1.11.

During the 1930s and 1940s, experiments with bubble rafts were carried out to illustrate the concept of packing of atoms and ions in a minimal energy configuration. It is interesting to see the hexagonal pattern formed from uniform-sized bubbles caused by the short-range order, which results in each bubble surrounding itself by neighboring bubbles. This remarkable order arises spontaneously and can be simply explained in terms of surface tension and capillary forces. The short-range structural arrangements are repeated throughout the raft, leading to long-range ordering. At Cambridge University in 1947, Bragg and Nye (34) generated monodispersed bubbles using a nozzle; this led to the preparation of a 2D bubble raft in which defects could be detected. From these studies the basics concepts of crystallization could be illustrated and it could also be demonstrated how grain boundaries, dislocations, lattice defects and recrystallization arise. Later, Smith (35) developed the method further and found these systems to be useful as models applicable to grain growth and the kinetics of phase separation. More recently, deformation experiments were carried out on 2D bubble rafts by Arciniaga and coworkers (36) in which two distinct transition or failure modes were detected; this corresponded to a brittle fracture at high

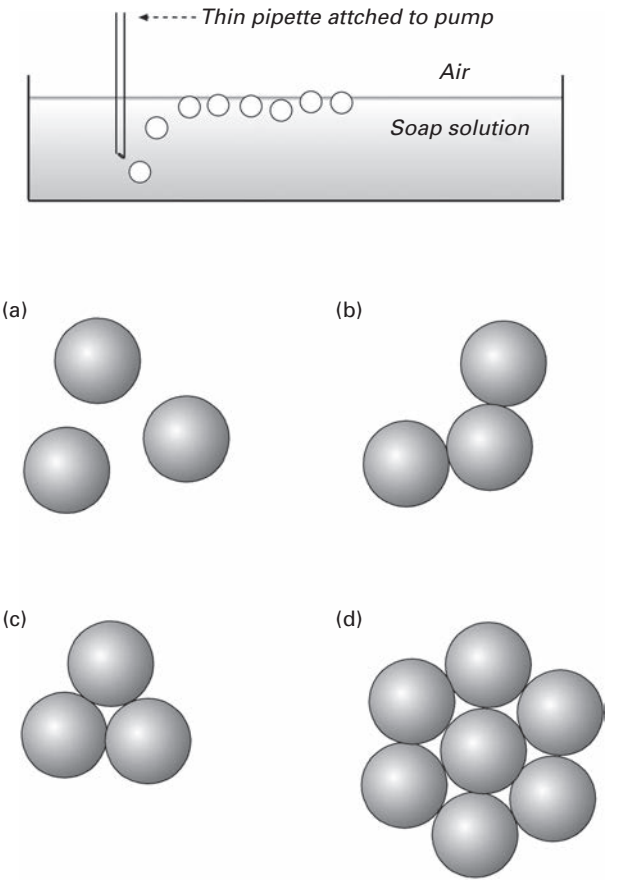

Fig. 1.11 The experimental set-up for the construction of a bubble raft and below typical bubble rafts with different configurations of monodispersed bubbles on the surface of the liquid: (a) three separate bubbles; (b) one possible packing of three bubbles – capillary forces will attract the bubbles together; (c) a lower energy packing of three bubbles; (d) hexagonal bubble packing. From ref (33).

deformations and plastic pinch-off under small deformations. This work was particularly relevant to the field of fundamental metallurgy. A typical bubble raft with dislocations and defects is shown in Fig. 1.12.

In order to carry out experiments with smaller bubbles, smaller nozzles and higher pressures were required, but it was found that the bubbles became less monodispersed due to hydrodynamic effects. This problem was solved by introducing a background circulation of the liquid which caused the rapid detachment of monodispersed bubbles. This approach eventually led to the development of flow focusing bubble generators and microflow bubble generators. More recently, the Physics Foam Research Group at Trinity College, Dublin (37, 38), prepared wet foam rafts from small (diameter 200 μm) bubbles using a solution of conventional commercial surfactant (a liquid detergent) and confirmed the observations made by Bragg and

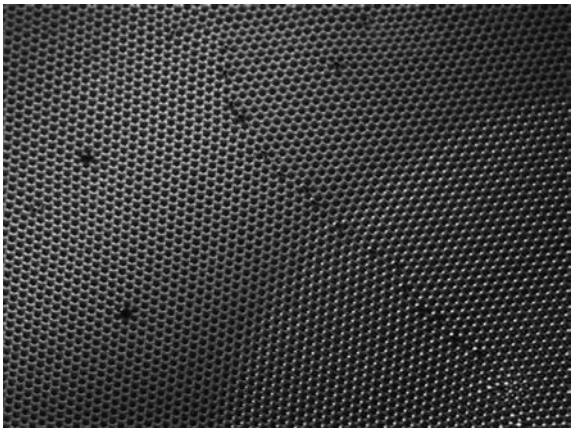

Fig. 1.12 A typical 2D bubble raft. Grain boundaries, dislocations, lattice defects and recrystallization can be detected. The short-range ordering is repeated throughout the raft, leading to a long-range structure packing which resembles the arrangement of closely packed crystals.

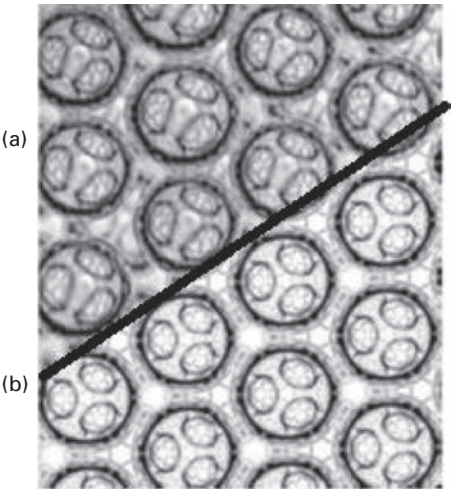

Fig. 1.13 (a) The ordered arrangement of a foam surface consisting of at least three layers of bubbles (mono-dispersed of size 200 micron) and (b) a simulation of a (111) face center cubic packing corresponding to the packing scheme ABC which shows detailed agreement with the experiment. From ref (37).

Nye in 1947 for 2D bubble rafts. These workers observed two different surface patterns of the top bubble layer which were described as triangular and square surface arrangements. In addition, they successfully developed techniques for preparing stable 3D wet assemblages which they could use to describe a rich variety of 3D crystal and defect structures. Also, computer simulations of these structures were made. These workers suggested that the stability and ordering of these structures (constructed from relatively large bubbles of about 200 microns) could not be explained by current thermodynamic and kinetic theories. In Fig. 1.13, a foam raft is shown consisting of bubbles giving an

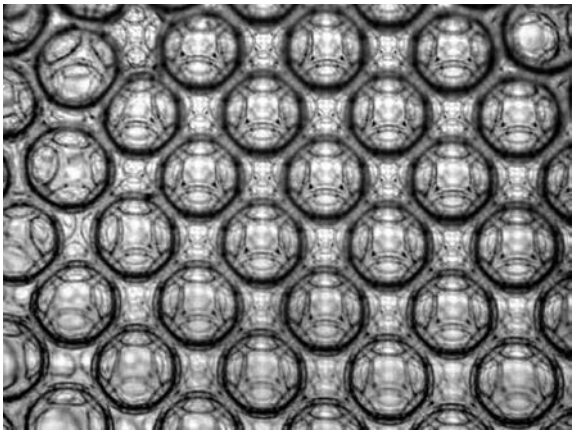

Fig. 1.14 Photograph showing at least five layers of bubbles arranged in a packing direction (100). Bubble diameter 0.5 mm. From ref (37).

ordered arrangement of at least three layers of bubbles which could be modeled as a (111) face center cubic packing arrangement.

In Fig. 1.14, a five-layer arrangement is shown, and sequences of up to seven-layer face center cubic planes were observed. In these structures, imperfections and stacking faults caused by point defects and vacancies of two bubbles (di-vacancies) were reported. In addition stacking faults similar to those found in opals were detected. In more recent studies, a flat-sided pyramid container that enabled ordered face center cubic single crystal foams of up to 500 bubbles to be produced was used. Also it was found feasible to produce strained and deliberately defective crystalline foam structures (38).

It has also been shown from recent experiments that bubbles of equal volume readily crystallize into ordered polyhedral structures when introduced into tubes where the width of the tubes has the same order of dimension as the diameter of the bubbles. Several characteristic structures have been identified experimentally and it was found that these structures tend to become generated in specific regions where the structure characteristics and dimensions are defined by the lower surface energy situation. Tobin and coworkers (39) carried out experiments with tubes with circular, square and triangular cross-sections and produced a variety of new ordered foam structures. The simple bubble generation apparatus is shown in Fig. 1.15.

In addition, computer simulations were carried out in which the surface energy per bubble was computed using the Brakke's Surface Evolver software (15). From these simulations the relationship between the energy per bubble and the characteristic tube width to bubble radius (defined as λ) was determined, where λ was varied by changing the tube diameter or bubble diameter. In Fig. 1.16, the dependence of surface energy on λ and the range of different ordered structures which could be generated are illustrated. The structures of the foams were labeled *S-N*, where *S* stands for square and *N* is the number of bubbles in the unit cell. Seven square structures were identified which could be simulated using the Surface Evolver. However, it was found that some of these simulated structures were hard to achieve experimentally.

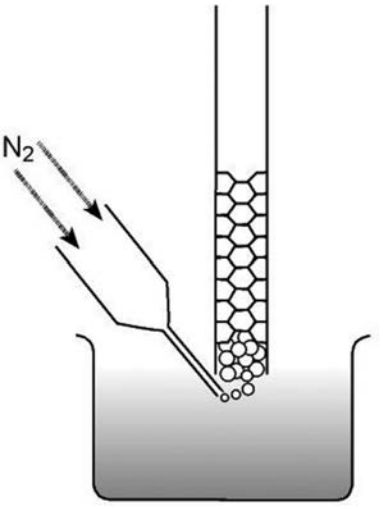

Fig. 1.15 Schematic representation of the apparatus used to produce ordered foam structures in tubes. Equal bubble volume achieved by having constant air flow is very important. From ref (39).

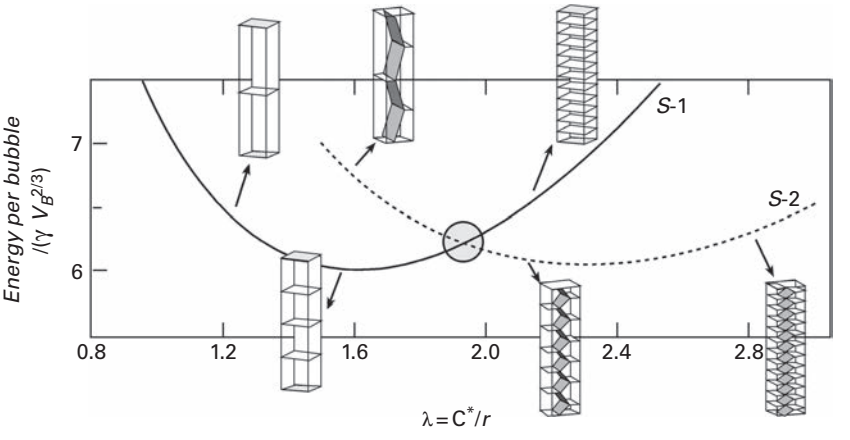

Fig. 1.16 The relationship between the energy per bubble and λ (defined by the characteristic tube width to bubble radius and calculated from $\lambda = c^*/r$) obtained from computation carried out using the Brakke's Surface Evolver software (15). Several different types of structure are shown, such as the bamboo structure at λ values less 1.9 and the staircase structures at higher λ values. However, the transition does not occur where the energy curves intersect but instead at $\lambda = 2.2$. From ref (39).

In addition, a series of experiments were carried out by Szekrenyesy and coworkers (33) in which 3D foams were produced by raft preparation techniques, with the aim of studying the stability of complex foam systems. The bubble rafts were constructed by releasing bubbles from an orifice which rose to the air/water interface in a temperature-controlled sealed cell which was designed to eliminate external disturbances (Fig. 1.17). These rafts could be classified as (a) a single bubble on the

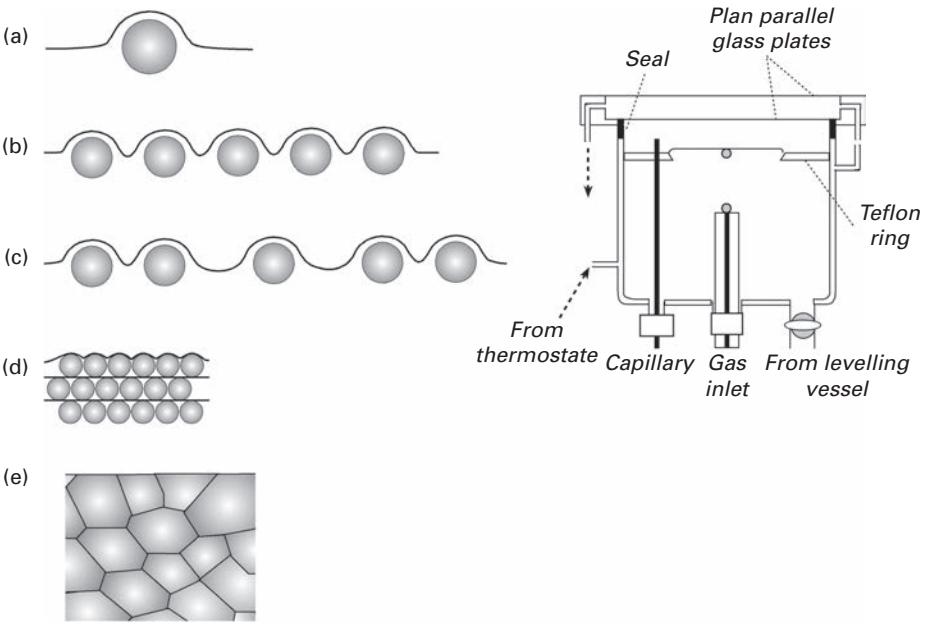

Fig. 1.17 Model foam systems (left) consisted of (a) single bubbles, (b) 2D foam in steady state, (c) 2D foam during decay, (d) three-bubble thick film, and (e) real foam and the apparatus for investigation of foam models. From ref (33).

surface of a liquid; (b) a 2D foam consisting of a one-bubble thick foam film on the surface of a liquid in the steady state; (c) the same system as (b) but in the state of spontaneous decay; (d) a three-bubble thick foam in its steady state; and finally (e) a thicker foam with similar features to a real practical foam, but not too far from its original state and structure.

For each of the models, the stability of the bubble rafts was investigated from a chemical approach by changing the surfactant and salt concentrations, the bubble size and the foam complexity. These experimental models clearly demonstrated the difficulties in simulating real foam systems. It was concluded that the dynamic processes involved the thinning of lamellae, elasticity of the surface layer, hydrodynamics and flow through the Plateau borders of different structure, gas diffusion, etc., were inter-related and could not be modeled as separate entities.

1.7 Foam structures produced from bubbles with wide size distributions

A simple approach to foaming can be demonstrated by bubbling air through a glass frit set in the base of a cylindrical glass column which contains an aqueous solution of soap. Bubbles with sizes larger than several microns rise to the surface fairly rapidly due to gravity, and the liquid is collected at the bottom of the column. The situation which develops is shown in Fig. 1.18.

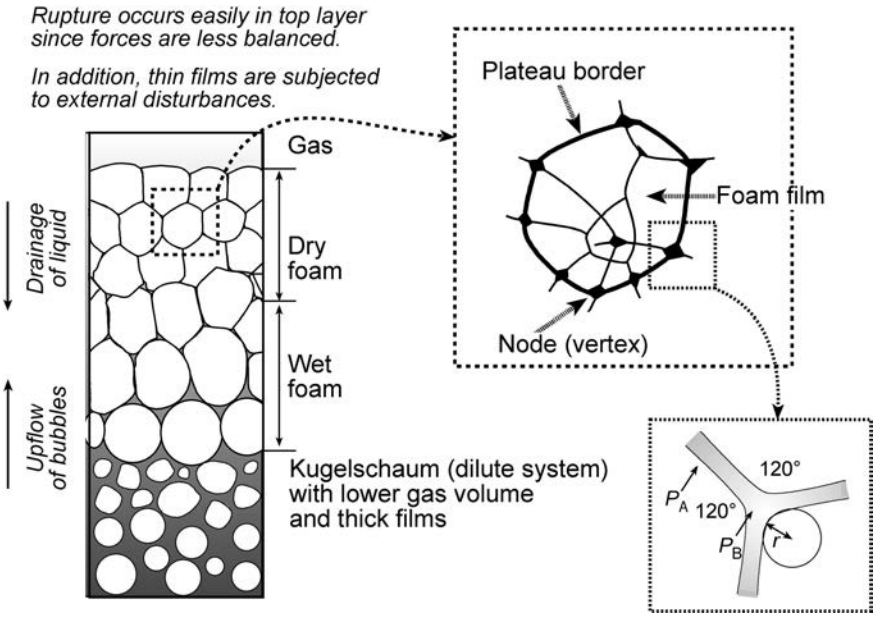

Fig. 1.18 The structures of foam occurring during formation and drainage of foam in a column. From ref (40)

In the foam column, several different transitional structures may occur with structures having high gas fractions near the top of the column, graduating to low gas content structures near the base of the column. The drainage of excess liquid from the foam column into the underlying solution is initially driven by hydrostatics, which causes the bubbles to become distorted. The pressure difference between neighboring cells (ΔP) is related to the radius of curvature (r) of the Plateau border by $\Delta P = 2\gamma/r$, as discussed in Section 1.4. The generalized model for drainage involves the Plateau borders subsequently forming a network, through which the liquid flows due to gravity. Foam collapse usually occurs from the top to the bottom of the column, and thin films in the kugelschaum (spherical) foam region are susceptible to rupture by shock, temperature gradients or vibration. Within the column, the two fairly well-known, easily recognizable, more or less extreme structures can be observed which have different degrees of wetness.

Overall, the foam may be considered as a temporary dilute dispersion of bubbles in the liquid, but when the volume fraction falls below about 30%, they transform from their spherical shape and distort into polyhedral gas cells with thin flat walls. The polyhedra are almost regular dodecahedra, and the junction points of the interconnecting channels are the Plateau borders. At any height in the foam column, the negative Laplace pressure in the Plateau borders is γ/r, and this pressure is balanced by gravity ($\rho g H_f$), so that the bubble size is related to the foam height by the equation

$$r = \frac{2\gamma}{\rho g H_f} \tag{1.4}$$

where H_f is the height of the foam above the bulk liquid.

1.8 Surface-active agents are needed to stabilize bubbles and wet foams

Since dry foams usually originate from bubbles which produce initially wet bubbly foams, it is important to begin this introduction by briefly surveying the history and basic physical chemistry of bubbles and wet foam systems. First of all, it is important to stress that bubble formation and foaming are not trivial processes. Essentially, foaming may be defined as a synergistic process where it is necessary to add a surface-active material (a third component to the air/water mixture). The presence of a surfactant entering the gas/liquid interface reduces the surface tension (lowers the interfacial energy) relative to that of the pure liquid. For example, water has a surface tension of 72.8 mN m^{-1} at room temperature and lowers to about 35 mN m^{-1} upon addition of a good surfactant.

Pure liquids of low viscosity, such as water, cannot produce wet foams unless a surface-active material is present. In fact, when a gas bubble is introduced below the surface of a pure liquid, it bursts almost immediately as soon as the liquid has drained away, and although bubbles can be generated or produced by ultra clean water, they last only a few milliseconds. A simple test for the purity of water can be made by vigorously shaking the sample in a closed glass container. The purity of the water is usually estimated from the bubble persistence time, and a bubble persistence of just one second on water is an indication of the presence of a surface-active impurity, such as dust. Hence, this bubble persistence can be used as a clear signal of impurities. However, some degree of stability can be achieved by slightly impure, highly viscous fluids (such as melted organic polymers) which sustain the thin film, and hence the foam structure, due to low drainage. Generally, the cleanliness of the system and the vessel can have an important influence on foaming.

1.8.1 The adsorption of chemical surfactants at the air/water interface

Since a surface-active foaming agent must be present in the aqueous environment to produce bubbles and foam, it is important to consider them in detail. The most common surface-active foaming agents are chemical surfactants, which can be considered to be partially soluble molecules, have some affinity for the air/water interface and are amphiphilic chemical molecules. They consist of a lipophilic tail which has a similar form (usually a long chain hydrocarbon) and a hydrophilic head group which consists of a range of different types of polar groups. These are two entities which are classified as hydrophobic (water-avoiding or hating group) and hydrophilic (water-preferring or loving groups) and they vastly differ in their solubility in water, which causes them to rapidly adsorb at the air/water interface. The hydrophilic head groups have a strong tendency to interact and solubilize in the water. The main types of surfactants are distinguished and characterized by the head groups: ionic (anionic or cationic of ampholyte) and nonionic. Several different types of surfactants structures are shown in Fig. 1.19.

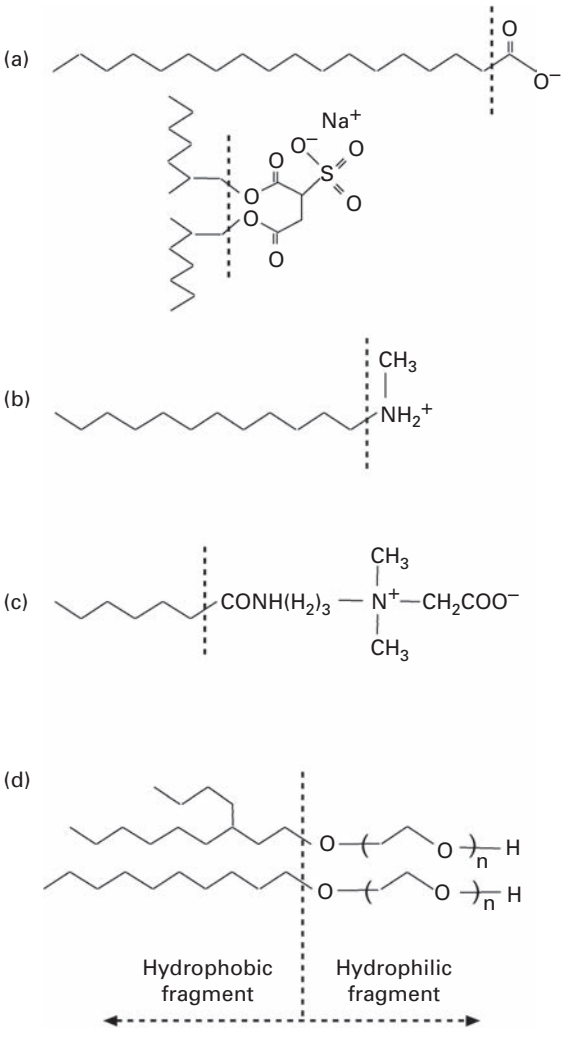

Fig. 1.19 Representative head-group structures of different surfactant classes; (a) anionic, fatty acid and sodium di(2-ethylhexyl) sulfosuccinate; (b) cationics; (c) a group of zwitterionic surfactants; (d) nonionic surfactants – alcohol ethoxylated branched and straight-chained.

The most common type of surfactants are the anionic surfactants, which may be expressed in the case of fatty acid by the formula $RCOO^{-}\,Na^{+}$, indicating its negative charged functional head groups. Cationic surfactants often have quaternary amine structures with the positive charge on the nitrogen atom and tend to adsorb on negative-charged surfaces (e.g., glass and silica and are considered to be poor foaming agents). Amphoteric surfactants exhibit both positive and negative charged groups, thus exhibiting zwitterionic properties, so that the charge changes with pH. Nonionic surfactants consist of hydrophilic head groups, and an important

Table 1.1 Commonly encountered hydrophilic groups in surfactants.

General class name	General solubilizing structure
Sulfonate	$R—SO_3^-M^+$
Sulfate	$R—OSO_3^-M^+$
Carboxylate	$R—COO^-M^+$
Phosphate	$R—OPO_3^-M^+$
Ammonium	$R—N^+R_xH_yX^-(x=1-3;\ y=3-1)$
Quaternary ammonium	$R—N^+R_3X^-$
Betaines	$R—N^+(CH_3)_2CH_2COO^-$
Sulfobetaines	$R—N^+(CH_3)_2CH_2CH_2SO_3^-$
Polyoxyethylene	$R—OCH_2CH_2(OCH_2CH_2)_nOH$
Polyoxyethylene sulfates	$R—OCH_2CH_2(OCH_2CH_2)_nOSO_3^-M^+$
Polyols	$R—OCH_2—CH(OH)—CH_2OH$
Sucrose esters	$R—O—C_6H_7(OH)_3—O—C_6H_7(OH)_4$
Polyglycidyl esters	$R—(OCH_2CH[CH_2OH]CH_2)_n—\cdots—OCH_2CH[CH_2OH]CH_2OH$

class are the alcohol ethoxylated branched and straight-chained surfactants. In Table 1.1 the most commonly encountered hydrophilic groups in chemical surfactants are listed.

Block copolymers of type A_nB_m, where A chains are hydrophilic and B are hydrophobic, are also surface active. There are many other common hydrophilic groups found in commercial chemical surfactants such as phosphates, betaines, polyethylene sulfates, and many different types of natural surfactants such as sucrose and glucose types which are manufactured from plant oils. Various modifications have been explored in the search for surfactants with improved functional foaming performance. Recent developments in synthetic surfactants include Gemini surfactants which consist of two lipophilic and two hydrophilic segments in the same molecule, with the two surfactant portions separated by a spacer which can vary in length. They give superior surface activity to conventional surfactants and, by adjusting the spacer length, they can be designed to give low or high foaming characteristics (41). A typical Gemini surfactant is shown in Fig. 1.20. Unusual heterogemini surfactants with two different chains and two different head groups have also been prepared.

Water is an unusual liquid in that it has a high surface tension (excess surface energy). This results from its characteristic tetrahedral hydrogen-bonded structure. Although the structure is not fully understood, it is generally accepted that weak fleeting hydrogen bonds link the individual water molecules in bulk solution, but the links are weak and do not completely break such that they experience symmetrical interactions in the surrounding environment and are attracted iso-tropically (equally in all directions). (42, 43). However, water molecules at the interface adopt a less balanced structural arrangement leaving some with unequal attractive hydrogen bonding arrangements, as shown schematically in Fig. 1.21(a). Although the standard model of water which was

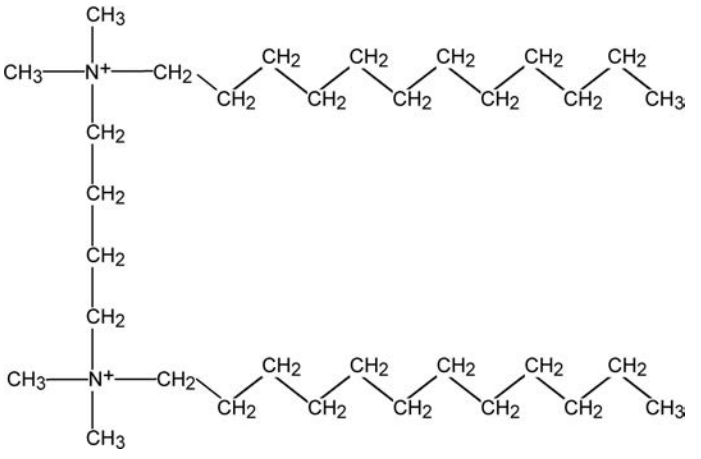

Fig. 1.20 The structural formula of a typical Gemini surfactant. The molecule is represented as 12-4-12; counterions have not been included.

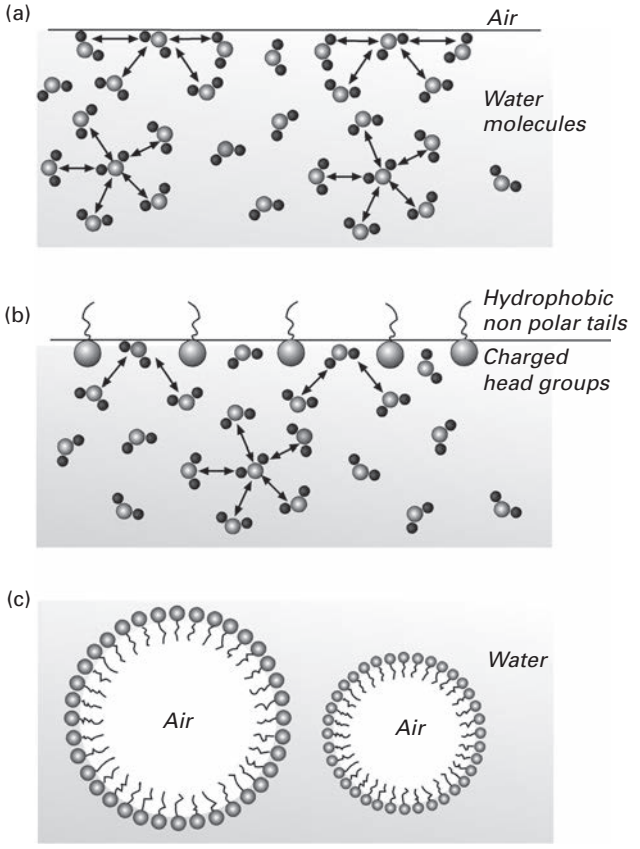

Fig. 1.21 The stabilization of bubbles in water by surfactants. (a) Water molecules are attracted to each other by fluctuating electrical forces, with molecules within the bulk liquid experiencing equal attractive forces in all directions, but molecules close to the surface experience unequal attractive forces and are attracted more strongly to the bulkl this causes a high surface tension (surface energy). (b) Adsorption of the surfactant molecule at the interface displaces some of the water molecules, causing a reduction in surface energy which acts to stabilize the interface. (c) Provided there is a sufficient concentration of surfactant at the interface, the bubble is stabilized by an elastic film.

originally developed from neutron scattering and computer simulations indicates that each water molecule is on average linked to four other molecules as a tetrahedral-like structure, this may not be the complete picture. Other more current theories have been proposed; for example, Pettersson and coworkers (44) used X-ray absorption and claimed that the molecules in liquid water bind on average to just two other water molecules, forming chains and rings.

To produce bubbles in water, a fresh interface is generated that results in a considerable amount of surface energy, and this may be resolved by the adsorption of surfactant. The process of adsorption of the surfactant is accompanied by the displacement of water molecules and a reduction in surface tension or surface energy. This is achieved by the accumulation of the hydrophobic groups at the interface which can either form hydrogen bonds or dipole bonds with water, and this is the basis of the mechanism by which soaps and detergents operate. In fact, soaps, detergents, lipids, etc., can reduce the effect by forming structural monolayers at the interface, exposing less polar functional groups to the air while presenting a more water-compatible surface to the bulk water as indicated in Fig. 1.21(b). This configuration increases the elastic nature of the interface and stabilizes the thin film which encapsulates the bubbles, as shown in Fig. 1.21(c). It is also important to note that the presence of surfactant can cause a change in the sign and magnitude of the charge on the bubble interface.

It is the manner in which the surfactant molecules align at the interface which determines the elasticity and stability of the film. Also, the presence of the net charge on the surfactant polar head group determines the surface activity. Essentially, the film formed by short-chain, low molecular weight surfactants (soaps) acts as an adsorbed fluid layer which may rapidly flow to regions with reduced surface concentration and repair areas of thinner film caused by fluctuations in film thickness from external disturbances. Surface-active high molecular weight polymers such as proteins also act as effective stabilization agents, but by a contrasting mechanism. In this case, they form a viscoelastic adsorbed layer which stretches and partially unfolds, stabilizing the bubbles. In many systems such as food foams, it is thought that there is a mixture of polymer and surfactant competing for the interface which may cause a weakening of the film. The two different stabilizing mechanisms can cause the low molecular weight surfactant to weaken the viscoelasticity of adsorbed protein film, and the polymer can act to retard the fluidity of the surfactant film.

1.8.2 The purity of chemical surfactants in foaming

Most surfactants are used as received grade, but often this is insufficient for reliable foaming investigations, because trace impurities often give rise to an increase in surface activity (by several orders of magnitude) higher than the purified surfactant. In academic laboratories, well-defined highly purified surfactant chemicals (homogeneous materials) are routinely used, but in industry most products are rarely pure and frequently contain mixtures of chemical isomers, residual solvents, unreactive materials and contaminants which effect foaming performance. Frequently, the impurities are a result of the

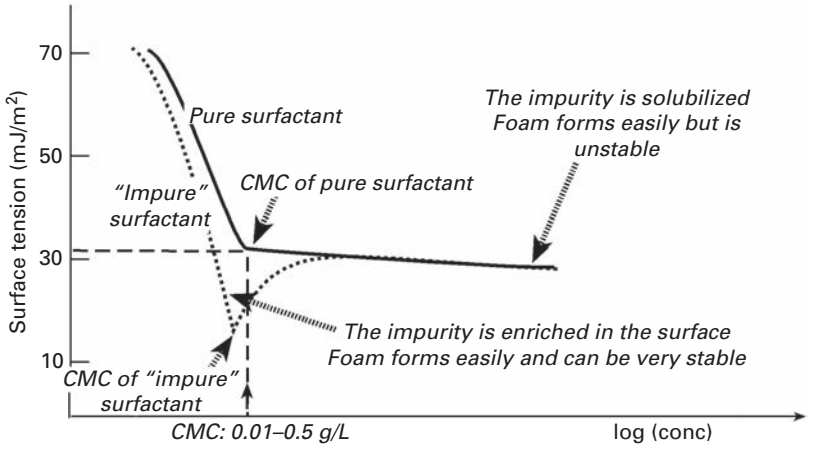

Fig. 1.22 Surface tension versus log (surfactant concentration) plots for pure and impure surfactants systems.

manufacturing process which may involve several steps. For example, in the case of sodium lauryl sulfate, surface tension data have clearly demonstrated that impurities and aging effects (caused by partial decomposition of the surfactant) have a profound influence on surface activity. Impurities frequently lead to confusion with regard to foaming data published. In fact, contamination can vary from batch to batch. Impurities may have a drastic effect on the adsorption kinetics and can influence not only the critical micelle concentration (CMC) and the micellar decay but also the foaming properties and surface tension. Lunkenheimer (45) discussed the chemical requirements on surfactant purity for performing reliable research and described the interfacial properties of several surfactants received from chemical suppliers. Stubenrauch and Khristov (46) reported on the influence of impurities on the stability of foam and foam films prepared from a series of cationic alkylmethylammonium bromide (C_nTAB) surfactants with different chain lengths. Characteristic surface tension versus log (surfactant concentration) plots for pure and impure surfactants systems are shown in Fig. 1.22.

1.8.3 Other types of surface-active materials

Such amphiphilic chemicals are not the only foaming agents as particles (partly hydrophobic), polymers, proteins and biomaterials also need to be considered which, due to their hydrophobic/hydrophilic balance, are also partially surface-active and able to adsorb at the air/water interface together with specific adsorbed cations or anions from inorganic salts. Many of these substances can cause foaming at extremely low concentrations (as low as 10^{-8} M). Sea foam is an interesting example of a weakly stabilized (transient) foam in which many different types of surface-active organic materials cause the generation of a foam which usually has a short lifetime, usually about 60 to 300 seconds. It is generated during strong winds and stormy conditions and the accumulation of different types of organic impurities

Fig. 1.23 Foam swept from the sea on to the road at Cleveleys, Lancaster, UK, January 1, 2012. From ref (49).

in the water act as surfactants often producing dirty froth-type foams which are frequently blown inland. Stormy conditions, high wind and high tides can easily churn up algae from the sea, and, as waves break ashore, air is trapped, forming bubbles. From photographic studies, the fractional coverage of the sea with foam has been recorded under differing conditions and a power law derived relating the coverage to the wind speed above the surface of the waves. It has also been reported that in the region below the foam layer, a continuous layer of bubbles exist. Theoretical studies by Newell and Rumf (47) related the magnitude of wind energy and momentum to the generation of waves and foam. It has been found that the generation and break-up processes are accompanied by the spraying of droplets of water into the air just above the surface of the waves. The thickness of foam layer and average bubble size has been estimated from the energy balance of the droplet and the energy input during formation. Two distinct mechanisms of bubble formation inside whitecaps were reported by Deane and Stokes (48). These occurred over different length scales, with the larger bubble produced from turbulent fragmentation and the smaller bubble generated by jet and drop impact on the wave. Occasionally, excessive foaming resulting in foams with longer term stability have been observed on inland roads near coastal waters (Fig. 1.23).

1.9 Surface tension and surface energy

Surface tension is the property of a liquid which enables it to stretch like an elastic sheet. It can be defined as the force acting to oppose the increase in the stretching or increase in surface area which occurs when we blow a bubble or stretch a liquid film. For example, if we stretch a soap film of length l_t on a wire frame over an infinitely small distance dx so that the relative thickness does not significantly change but remains thick enough to prevent overlapping of the interfacial regions,

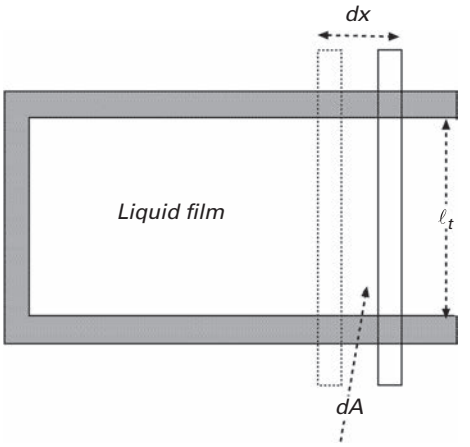

Fig. 1.24 Schematic set-up showing the increase in surface area against an opposing tension.

then a significant amount of work is required to prevent the film from pulling back and reversing the process. In fact, the surface of a liquid may be considered as a stretched skin where force or work is needed to prevent the process from reversing. The stretching process involves an increase in surface area, and the amount of work dW which has to be done to achieve this must be proportionate to the increase in surface area dA, as indicated in Fig. 1.24.

However, since the film has two surfaces, the surface area doubles (2 dA) and this is equivalent to $2dx\,l$, and since the change in surface area is proportionate to the amount of work, we may express this balance by the equation

$$dW = \gamma dA \tag{1.5}$$

where γ is defined as the surface tension and for a significant larger change in surface area (A) then

$$\Delta W = \gamma \Delta A \tag{1.6}$$

The surface tension can also be defined as the force F that is equivalent to the amount of work that has to be done to increase the liquid surface area. Hence, the term surface tension F can be expressed in the form

$$F = -\frac{dW}{dx} = -2\gamma \ell_t \tag{1.7}$$

The dimensions of surface tension mJ m^{-2} are equivalent to those of surface energy mN m^{-1}.

In general terms, it is also possible to consider the surface tension as a tension applied to a rubber balloon where a force increases the surface area against a tension. However, the expansion of liquid surface is a plastic process while the stretching of rubber membrane is elastic. Surface energy can also be understood at a molecular level, as

the work required to bring molecules from inside the bulk liquid to the newly created interface. Since these molecules on reaching the interface become only partially surrounded by other molecules, this causes an energetically unfavorable situation due to kinetic and steric restrictions that require energy, which may be expressed in terms of the van der Waals forces, and re-arrangement of hydrogen bonds.

1.10 Gibbs adsorption and Gibbs elasticity

Gibbs realized that the adsorption interface was not as a sharp mathematical surface and introduced the surface phase as a layer with a small but finite uniform thickness which contained a surface excess of adsorbed molecules. This layer covers the homogeneous bulk phase. The phases are considered to be in thermodynamic equilibrium. According to the Gibbs adsorption theory (50), in 1878, in a binary system consisting of solute (component 2) and solvent (component 1), the adsorption of the solute is defined in terms of the excess molecules of solute (per unit area of the liquid surface) compared to the amount in bulk solution. The quantity of the excess solute adsorbed at the interface can be quantified by choosing a dividing plane such that the adsorption of component 1 is zero. This gives a value of the relative adsorption of component 2 which is normally expressed as the surface excess $\Gamma_2^{(1)}$ as shown:

$$\Gamma_2^{(1)} = -\frac{1}{R_g T}\frac{d\gamma}{dlna_2} \tag{1.8}$$

where a_2 is the activity of the solute in bulk solution. Since the surfactant concentration in bulk solution below the CMC is normally low, the solute activity can be replaced by the solute concentration c_2, and we have the approximate expression

$$\Gamma_2^{(1)} = -\frac{1}{R_g T}\frac{d\gamma}{dlnc_2} \tag{1.9}$$

Most foam systems are stabilized by chemical surfactants and the Gibbs equation is very useful since it links the quantity of adsorbed surfactant at the air/water interface to the lowering in surface tension and temperature. As the solution concentration of the surfactant molecules is increased, the amount adsorbed at the interface also increases, and this causes a decrease in surface tension. It is of interest to note that the surface tension only slightly declines when the maximum occupancy of the surfactant at the air/solution interface is less than 60%, but a steep decrease occurs when the occupancy reaches about 80% (51).

Experimental measurements of γ over a series of concentrations enable a plot of γ versus $ln\ c_2$ to be constructed, and hence the adsorption density of the surfactant at the interface can be determined at different bulk concentrations of surfactant. Also, from the Gibbs adsorption equation, the value of $d\gamma/dlnc$ at any point on the curve corresponds to values of the surface head group packing density at the air/water interface. At increasing surfactant concentrations, the decline in slope reaches a limiting value, due

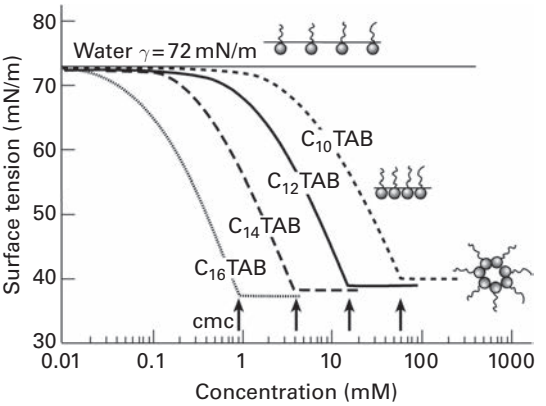

Fig. 1.25 Surface tension versus concentration for aqueous solutions of a series of long-chain amines. From ref (52).

to the self-aggregation of monomer units in bulk solution which leads to micelles, and this point is known as the "critical micelle concentration" (CMC) of the solution. Beyond this point, a sharp transition occurs and there is no further adsorption at the interface. For a series of medium-chain amines in water, the surface tension versus the logarithm of concentration plots are shown in Fig. 1.25. Interestingly, the chain length has almost no effect on the slope of the curves and this result suggests that the adsorption excess or surface excess is independent of the length of the chain and that the molecules have a similar molecular ordering at the interface, where the polar groups are directed toward the water and the non-polar toward the air.

The identical slope of the curves in Fig. 1.25 also suggests that the amines have the same surface area per molecule (A_2), and this quantity can be related to the adsorption by the equation

$$\mathrm{A}_2 = (1/\Gamma) \times 6.023 \times 10^{20} \tag{1.10}$$

where Γ is expressed in mM/m^3, and from the slopes of these curves the adsorption density can be calculated. Gibbs also considered the foam films as an elastic membrane and discussed the importance of surface elasticity (pull-back when stretched) in terms of the ability of the thin film to resist excessive localized thinning. This can be caused by minor mechanical shocks which would otherwise cause rupture. The Gibbs coefficient of surface elasticity was defined by E_G as equal to the stress divided by the strain per unit area and is a quantitative measure of the ability of thin film to adjust itself in instances of stress. It acts as a variable resistance to surface deformation during thinning and relates to the increase in surface tension for a unit of relative increase in the surface area and can be expressed by the equation

$$E_\mathrm{G} = 2\left(\frac{d\gamma}{d\,\ell n\, A}\right) = -2\left(\frac{d\gamma}{d\,\ell n\,\ell_\mathrm{t}}\right) \tag{1.11}$$

where $d\ lnA$ is the relative change in the surface area A and $d\ \ell n\ \ell_t$ is the relative change in the lamella thickness. The negative sign originates because if A is stretched to $A + dA$ then the film thickness decreases to $l - d\ell_t$. Because the thin film has two surfaces, the stress is equal to twice the increase of surface tension, where the factor 2 is introduced in the RHS of the equation. Basically, E_G is the quantitative measure of the ability of a film to adjust its surface tension in an instant of stress and needs to be relatively large for the film to remain stable. It may be considered as a measure of the resistance against the creation of a surface tension gradient. By combining Equation (1.11) with the Gibbs adsorption isotherm equation it can be shown that E_G is proportional to Γ, the surfactant adsorbed in the thin film

$$E_G = -(d\gamma / d\ ln\ \Gamma) \tag{1.12}$$

E_G is also related to the surfactant gradient. Two major variables which effect E_G are the film thickness and the concentration of surface-active material (the concentration gradients). In the simpler case described above where E_G is used to describe purely the elasticity, E_G is sometimes referred to as the "film elasticity of compression modulus." In the more general case (as covered in Chapter 7) where the surface behavior has both an elastic and a viscous component and is applicable to practical systems, then E_G is termed the "surface dilational (compression) modulus."

In Fig. 1.26, a thin film is shown where an external disturbance results in an increase in surface area (due to curvature) caused by a deformation. In the curved region, the surfactant is depleted from the surface, resulting in an increase in surface tension. The thin film at this moment is under Gibb's elastic stress and, to compensate, a flow of

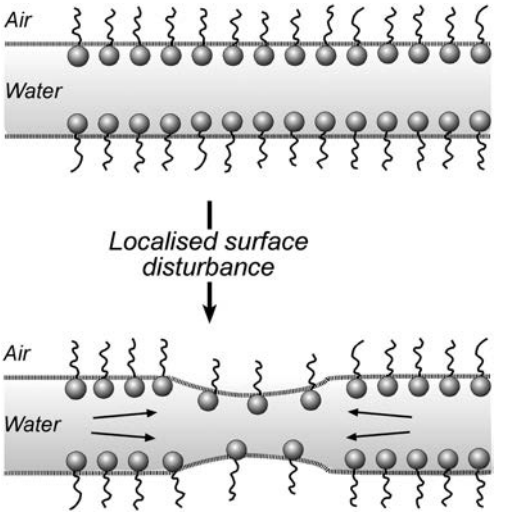

Fig. 1.26 Gibbs elasticity results from an external disturbance which causes deformation of the thin film and results in an increase in surface area and an increase in surface tension in the curved regions due to the depletion of surfactant.

liquid occurs which reverses the thinning process (the Marangoni effect) and repairs the film, so that it remains stable.

However, it is important to note that the Gibbs theory (50) only applies to a hypothetical equilibrium state (i.e. it is assumed that there is insufficient surfactant within the film to diffuse to the surface and lower the surface tension). Clearly, for thick lamellae, under dynamic conditions, the Marangoni effect (53) becomes important and operates on both expanding and contracting films. The Marangoni effect tends to oppose any rapid displacement of the surface (the Gibbs effect) and may provide a temporary restoring or stabilizing force to vulnerable thin films which can easily rupture. In fact, the Marangoni effect is superimposed on the Gibbs elasticity, so that the effective restoring force is a function of the rate of extension, as well as the thickness. In many situations, small accidental changes in surface area cause the surface tension to rapidly change, and the film thickness responds by a speedy adjustment, allowing the foams to retain their stability. Surface tension gradients are essential, and because E_G is the measure of the ability of a film to adjust its surface tension in an instant of stress, it should be relatively large *for freshly produced foams to survive.* It has been shown that E is proportional to $(d\gamma/dc)^2$, where c is the concentration of the surfactant in the thin film (54).

It is also important to consider the simplified system where E_G is used to describe only the elasticity; then E_G can be termed the "film elasticity of dilational or compression modulus." Such a situation occurs only for pure elastic interfaces, where the dynamic interfacial tension response $\gamma(t)$ follows the area change A (t) without any phase difference. Usually, in real situations, two major variables affect E, and these are the film thickness and the concentration of surface-active agent. Both influence the concentration gradients. In general, the interfacial tension follows the area change with a certain delay due to the various relaxation processes within the interfacial layer and between the interface and bulk solution. In this more general case, the surface behavior is complex and E has both elastic and viscous components.

1.11 Methods of measuring surface tension

Clearly, foaming is related to surface tension, and the foam-generating power of a surfactant solution is generally favored by the ability of a surfactant to attain a low surface tension within a short time. The surface tension of the foaming solution gives a measure of surface activity and, in the majority of foaming studies, one begins by examining the change in surface tension with respect to change in solution properties such as concentration, temperature and pH. All these parameters cause large variations in surface tension, which can be related to foaming performance. It is also important to consider the time scale of the adsorption process (and the rate of build-up of surface activity) since the diffusion kinetics of the surfactant molecules play an important role in the foaming. As the solution is shaken, the area of the interface is drastically increased, and although fresh bubbles are initially free of surfactant, the molecules are rapidly transported from solution to protect the film.

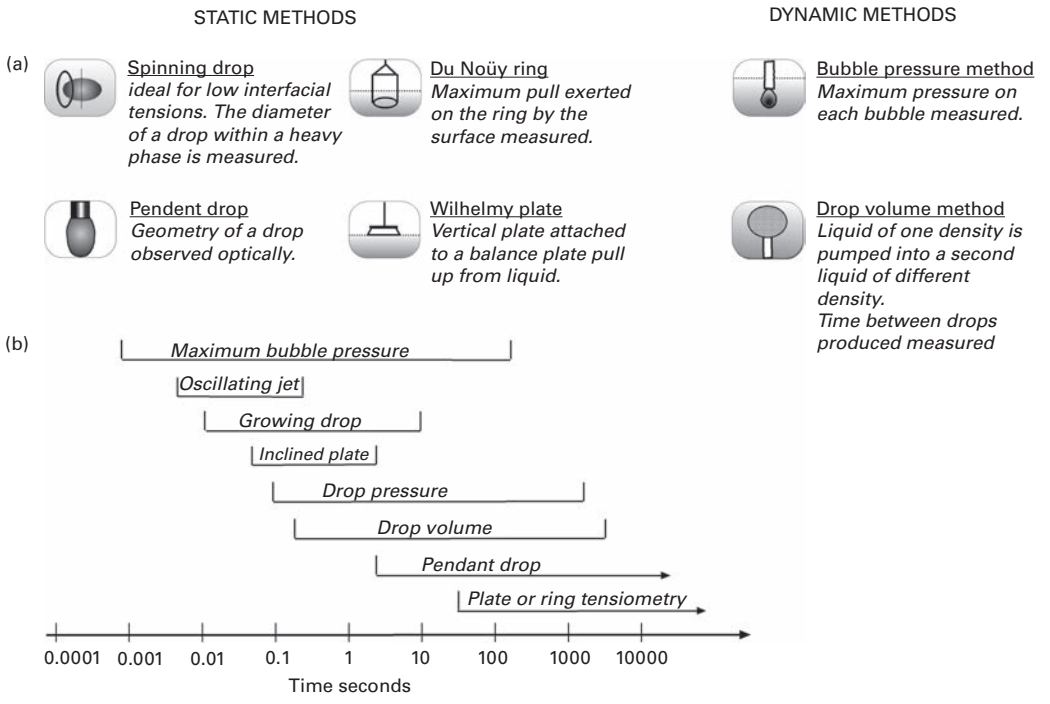

Fig. 1.27 Different dynamic experimental methods for measuring surface tension covering a wide range of time scales. From ref (56).

The adsorption of surfactant on an expanding interface has been extensively studied using a range of experiment techniques in which a fresh bubble on drop interface is created as a function of time. These different methods generally cover different time frames from milliseconds to hours or days. Prins (55) divided these dynamic techniques into two groups: (a) operating close to equilibrium or (b) far from equilibrium conditions. When laboratory measurements are carried out over the minute time scale or longer, they are frequently referred to as equilibrium methods and shorter time scales as kinetic methods. The equilibrium values of surface tension are lower than the dynamic values. Details of these methods have been well documented in the literature and a classification of the different methods used to measure both the static and dynamic tension of liquids is shown in Fig. 1.27, with estimated values of these different time ranges.

Probably the most convenient laboratory techniques are the equilibrium methods which involve the detachment of a ring or plate from the air/solution interface. For example, in Fig. 1.27, it can be seen that whereas the ring tensiometry method (Du Noüy) and the plate tensiometry technique measure over the range from about 15 seconds to several hours, the drop volume and drop pressure extend down to fractions of seconds. The kinetic methods such as the maximum bubble pressure method and oscillating jet are capable of operating over much more rapid time scales and, in recent years, modification of the maximum bubble pressure technique has enabled the equipment to become commercialized.

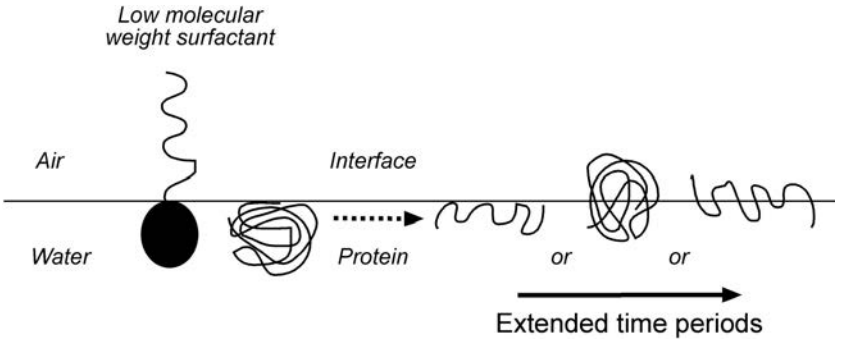

Fig. 1.28 Differences in adsorption behavior at the interface of (a) a low molecular weight long-chain surfactant which rapidly adsorbs and (b) a high molecular weight flexible protein polymer such as β-casein in which configuration changes may occur over extended periods of time.

Dynamic surface tension is particularly relevant for industrial processes which frequently occur under rapid shear; for example, high-speed printing, beating in food processing or shaking in detergency. However, the ability to achieve low values of surface tension over short times does not always correlate with the process since the surface tension may vary with location at the interface as well as with time variations. Also, problems may result during measurements due to the fact that when the surface is rapidly created (in less than 1 second) it is difficult to control the convective liquid motion. In some systems, especially with high molecular weight polymeric surfactants, the approach to equilibrium surface tension is usually very slow and in some cases may never be obtained, and this may be due to several reasons. For example, the configuration of polymer at the interface may change with time or the system may contain more than one solute and competitive adsorption may result from different species. In Fig. 1.28, the differences in adsorption behavior over time between a low molecular weight surfactant and a high molecular weight polymer are illustrated.

In the case of a fairly high molecular weight polymer (ethyl hydroxylethyl cellulose) (MW = 100,000 *Da*), values of surface tension (determined by the du Noüy ring method) were measured at varying concentrations over different time scales from fractions of a second to almost 20 min, which were considered to be relatively static conditions (57). The molecular structure is shown in Fig. 1.29 and the results are expressed as adsorption isotherms in Fig. 1.30; these relate the surface tension to the aging periods. Three distinct regions could be identified as consisting of an induction period, a fast fall region where the surface coverage occurred fairly rapidly and finally a meso-equilibrium region, and the results alsoare discussed in terms of the rates of adsorption and configuration changes of the polymer at the interface.

Proteins also adsorb slowly at the bubble surface and by acting as a surfactant cause foaming. The structure and stability of food foams produced from whey or egg white protein change within minutes. It is the natural flexibility within the molecule that can expose previously buried hydrophobic parts to the interface, thus resulting in the strong attachment

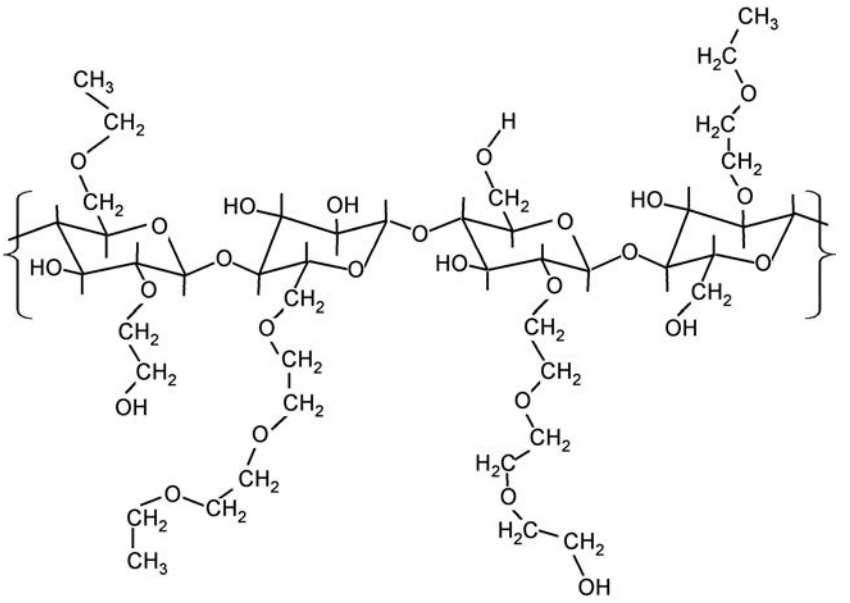

Fig. 1.29 Structure of the polymer ethyl (hydroxylethyl cellulose) ether.

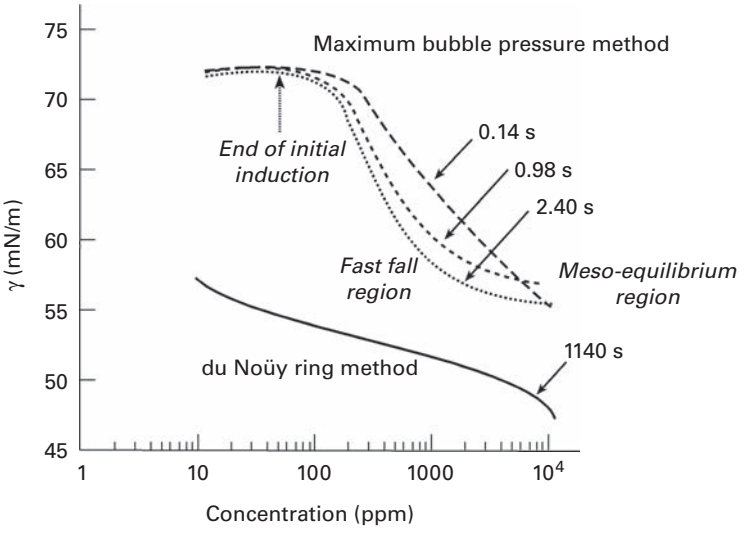

Fig. 1.30 The dynamic surface tension versus concentration for the polymer ethyl (hydroxylethyl cellulose) ether (molecular weight 100, 000). Surface aging times as indicated and method of measurements. The maximum bubble pressure method is used for the short-time aging and the du Noüy ring technique for extended aging. From ref (57).

forces. Generally, in these types of foaming studies, both dynamic and static data are informative since they provide complementary information. In the following sections the measurement of some established dynamic surface tension measurement techniques on freshly generated, expanding interfaces are discussed with relevance to foaming.

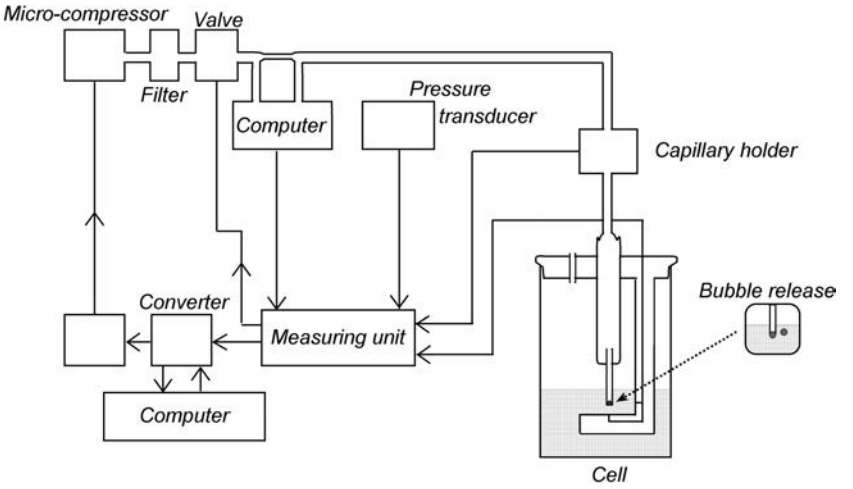

Fig. 1.31 Maximum bubble pressure method for measuring the dynamic surface tension equipment of surfactant solutions.

1.11.1 Maximum bubble pressure technique

Another important technique used to determine dynamic surface tension is the maximum bubble pressure method in which nitrogen bubbles are released from the tip of a single capillary immersed in the surfactant solution and the maximum bubble pressure for each bubble is measured using a sensitive pressure sensor. As the bubbles grow in size, the pressure increases until a maximum bubble pressure is reached which corresponds to the minimum radius curvature for the bubble (which occurs as it develops a hemispherical shaped). The method has been fully commercialized, and the set-up of the MPT2 model instrument (Lauda Instruments) is shown in Fig. 1.31.

To calculate the dynamic surface tension, we can consider that in generating the bubble work is done against the surface tension and the hydrostatic pressure so that

$$\Delta P = \rho g H_{im} - \frac{2\gamma}{r} \tag{1.13}$$

where ΔP is the capillary pressure, γ is the surface tension and H_{im} is the immersion depth of the tube orifice. This equation is based on the Laplace–Young equation, and measurements can be carried out as a function of time by using different gas flow rates.

1.11.2 Overflow cylinder technique

The overflow cylinder is another important dynamic method in which a solution of surfactant is pumped from a reservoir below a vertical cylinder to the top where it overflows from the rim to produce a thin vertical film on the outer wall of the cylinder. As the liquid proceeds to flow downward along the outside of the cylinder, it

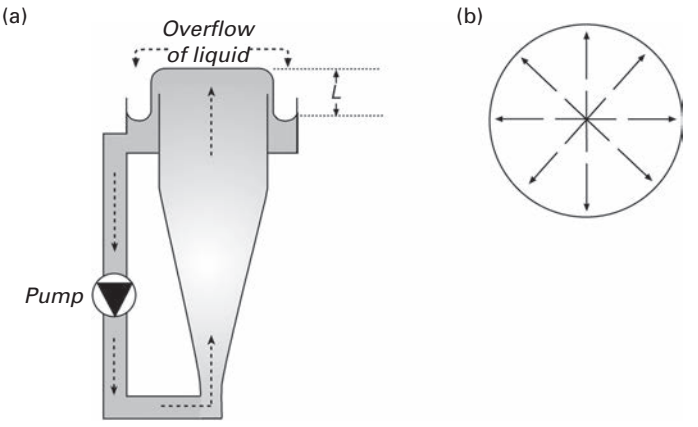

Fig. 1.32 Cross-section of an overflowing cylinder showing (a) the height L of the falling film at the outside of the cylinder and (b) the radial movement of the surface at the top of the cylinder. From ref (58).

is collected in the base of the cylinder and is recirculated by the pump. The equipment is shown in Fig. 1.32.

The expansion of the surface produces a radial movement on the surface and a surface tension gradient. The surface velocity increases linearly with the distance from the center of the cylinder. In this way, a radially expanding liquid surface is formed at the top of the cylinder and the expansion rate can be adjusted by changing the height of the falling film at the outside wall of the cylinder. The expansion rate of the surface ($dlnA^{-1}$) is usually measured by observing small talc particles floating on the expanding surface and recording their movement under known time intervals. The dynamic surface tension of the constantly expanding interface is measured near the center by a Wilhelmy plate and the equilibrium surface tension γ is measured on the surface in the inner cylinder in the absence of liquid flow. From these measurements, values of the surface dilational viscosity η_d can be calculated as

$$\eta_d^2 = \frac{\gamma_{dyn} - \gamma_{eq}}{d(lnA)/dt} \tag{1.14}$$

where γ_{dyn} *and* γ_{eq} are the dynamic and equilibrium surface tensions. In this experiment, the resulting expansion of the liquid surface is purely dilational and consequently free of shear effects. Several studies have been carried out by Prins and coworkers (59) under far from equilibrium conditions and the data was related to the foaming performance of industrial foams (foaming of a detergent or the efficiency of a plant spray). Experiments show that the increase in foamability appears to parallel the lowering of the dynamic surface tension but not the equilibrium surface tension (as shown in Fig. 1.33), which remains almost constant in the same concentration range.

Prins and Bergink-Martens (57) also showed that the dynamic surface tension of an aqueous solution measured using the overflowing cylinder method could be related to

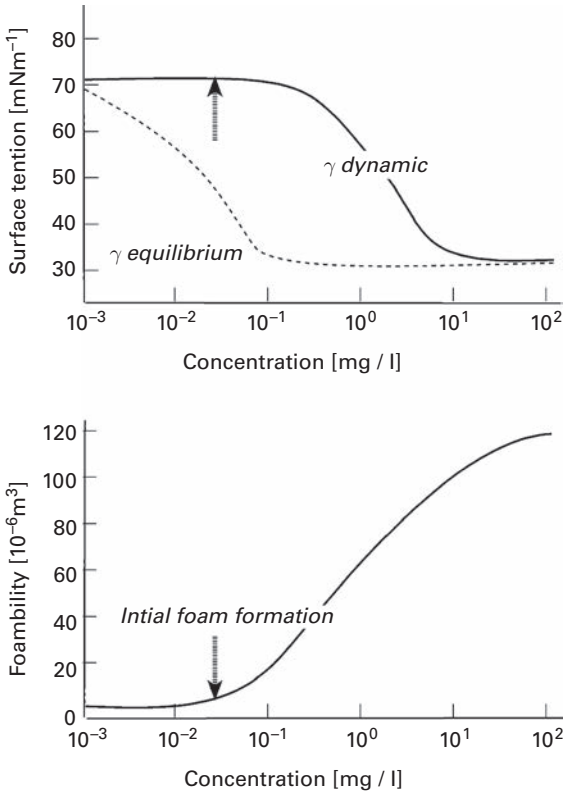

Fig. 1.33 (a) The equilibrium and dynamic surface tension of detergent solution (Teepol) and (b) the foamability versus concentration curve. The dynamic surface tension (measured using the overflow cylinder method) is shown to correlate with foamability. From ref (55).

foaming behavior, and this appears to confirm the relationship between dilational surface behavior and stability. The correlation was explained by the fact that during the generation of foam, liquid flows downward through the thin films (which exist between bubbles and Plateau borders) causing surface tension gradients which are similar to those induced at the surface of a free falling film. In fact, generally the film stretches as the liquid flows downward, decreasing the stability; since the adsorbed amount of surfactant decreases during this process, the surface tension increases in the upper parts of the film.

Another technique which has been used to obtain dynamic surface tension data involves a flat surface which is subject to a dilational disturbance by a moving barrier in a Langmuir trough. In foams, when bubbles are flowing in a liquid, a similar situation occurs since part of the surface is expanded, although another part of the surface may be compressed in such a way that these two parts of the film are interconnected. In cases where the whole bubbles are subjected to an applied expansion, other dynamic surface tension methods such as the Langmuir trough rather than the overflowing cylinder may be more relevant.

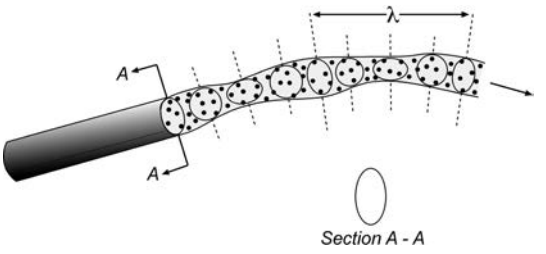

Fig. 1.34 Fluid emerging from a non-circular orifice showing a number of oscillations (surface tension values corresponding to various ages of the jet).

1.11.3 Oscillating jet technique

The oscillating jet method is an extremely rapid technique and involves forcing a stream of liquid through an orifice, so that it emerges as an oscillating jet with the cross-section area of the jet changing with distance from the orifice. The shape of the jet is originally elliptical, but due to the restoring momentum (produced by the surface tension forces) the jet reverses to a preferred circular shape. However, it then overshoots, producing another elliptical cross-section with major and minor axes reversed from the original configuration. This deformation process is rapidly repeated and is dependent on the surface tension, the density of liquid and size of orifice. Eventually, the jet appears stationary for the entire length before break-up occurs, and this allows precise measurements of the features of the jet (amplitude and wavelength) to be measured. The data can be used to deduce the properties of the surface tension as a function of distance from the orifice.

The original technique and theory were derived by Lord Rayleigh, but in recent years correction factors and modifications have been made to the original equations. It is of interest to note that Lord Rayleigh reported the surface tension of a soap solution within 1/100 of a second of its formation with a value close to water (60). Fig. 1.34 shows the fluid emerging from the non-circular orifice producing a series of oscillations, and in Fig. 1.35 the front and side images of an oscillating jet are shown.

In addition to aqueous solution of surfactants, the oscillating jet method has been used to determine the surface tension of an ultra-pure alloy (a molten Sn/Pb solder alloy) which is used in an assembly of microelectronic components (61). A reservoir was filled with solder pellets which are heated to liquify the alloy and the fluid was then fed to the jet. Experiments were carried out at high temperatures, and the equipment is shown in Fig. 1.36. This method of measuring dynamic surface tension is important for understanding the foaming behavior of metallic systems.

1.12 Foamability and foam stability

Although there is no standard coefficient of foaming, foams are characterized by their foam ability and their foam stability. The *foamability*, which is sometimes referred to as

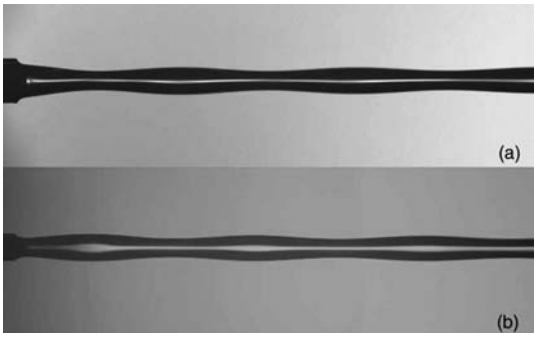

Fig. 1.35 Oscillating water jet: (a) front view and (b) side view.

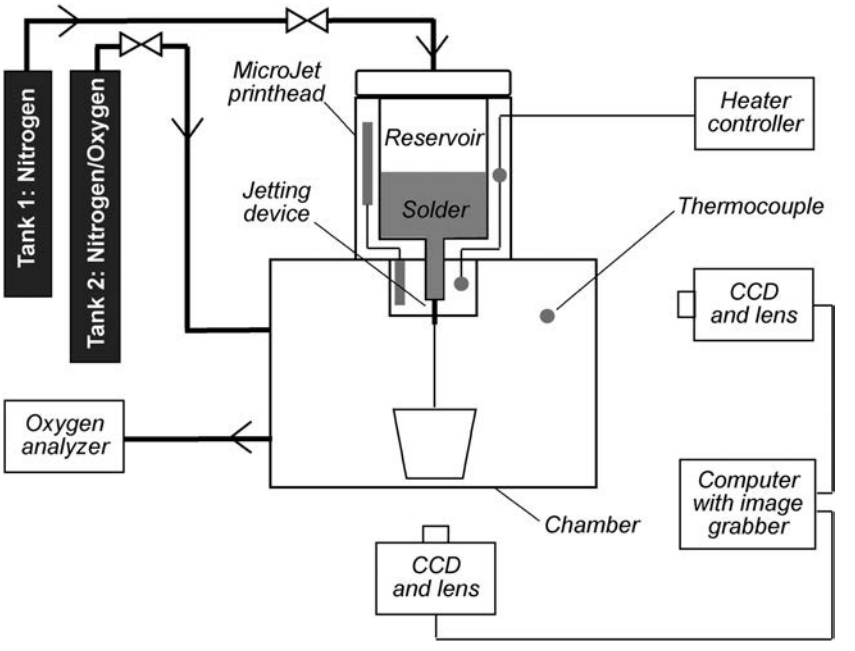

Fig. 1.36 Oscillating jet apparatus constructed for measurement of surface tension of ultrapure alloy. From ref (61).

foaminess or foam capacity is the quantitative assessment of the initial original foam height or volume (this is usually measured during steady-state conditions within seconds after completion of the generation step and entirely depends on the method of generation). The second step relates to the lifetime of the foam (after the generation or agitation step has been completed) and this is called the *foam stability*. From these tests, no detailed information on the foam properties (such as the liquid content or degree of wetness of the foam, the size distribution of the bubbles or the thickness of thin film lamellae) is revealed. Different foam systems may undergo different transitional structures in the decay process due to different types of stabilization/destabilization mechanisms.

This type of information can only be obtained from more detailed testing. The evaluation of foamability and foam stability also strongly depend on the method of foam generation and a convenient method of characterizing a surfactant system is based on the Ross–Miles test (62). This standard test method involves releasing a falling or plunging jet of the foaming solution from a pipette which impinges on another portion of the test solution below, creating mixing. Gas becomes incorporated and entrained when the liquid jet enters the free surface, and both the foamability (the initial build-up of foam) and the foam stability (the amount of foam remaining stable after a well-defined period of time) can be measured using this test. The method is important in evaluating many different types of surfactant types and is particularly relevant to foaming in kitchen and bathtub and situations involving the rapid flow of liquids over weirs or waterfalls. The method is described in further detail in Chapter 11 and a sketch of the vessel is shown in 1.37 (a). The data from different surfactant systems can be classified in five regions in terms of both foamability and foam stability according to this test method (Fig. 1.37 (b)).

Foamability and foam stability are interrelated, and it is the balance between these two parameters which defines the effectiveness of the surfactant for a specific application. Often, surfactants which give high foamability also give high foam stability. However, this is not always the case, since high molecular weight proteins and surface-active particles often show very low foamability and high foam stability. Usually, with mixtures of surfactants, it is possible to achieve high foamability with high foam stability, but in other cases high foamability with low foam stability occur

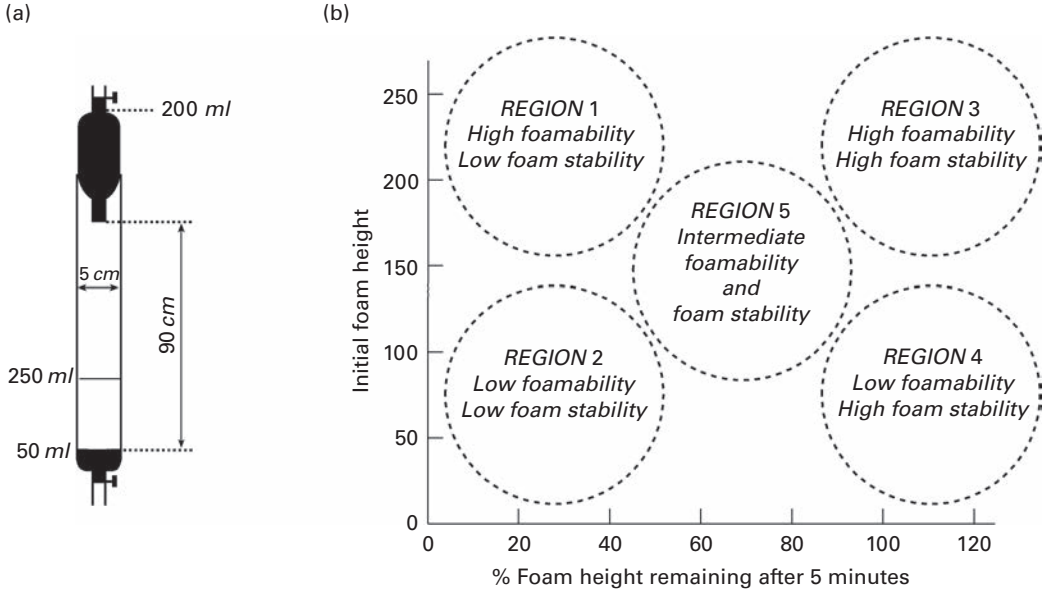

Fig. 1.37 (a) The Ross–Miles test apparatus enabling foaming to be classified by foamability and foam stability. (b) The classification of surfactant systems into five regions depending on the foamability and foam stability as determined by the Ross–Miles test apparatus. From ref (63).

and it is frequently difficult to differentiate between the different mechanisms involved. Also, it may be noted that foam generation is a dynamic test whereas foam decay may be rapid (immediately after generation) or slow (quasi-static in the case of long-lived foams) and is usually more dependent on the surrounding environment such as humidity and external disturbances (from pressure or temperature changes or evaporation). In addition, during foam decay, structure changes may occur. For low stability foams, drainage occurs after generation, but this tends to induce surface tension gradients at the interface of the lamellae which would tend to retard the drainage, and hence the rate of decay may be significantly reduced. It is therefore important to express the decay time as an average value.

It would appear that the method used in manufacturing the foam may also play an important role in defining the foamability/foam stability balance. While mild hand-shaking, the Ross–Miles method or the Bikerman method as described in Chapter 11 may be regarded as relatively low-energy foaming techniques, it has been established that high-energy foaming techniques such as microfluidic techniques are useful for generating foams from many amphiphile/particle mixtures. Arriaga and coworkers (64) used a microfluidic technique to study the foaming characteristics of a mixture of a short-chain amine (*n*-amylamine) and silica nanoparticles at a range of particle concentrations and amine concentrations. In the case of a dispersion of fairly high silica particles (10 w%) at amine concentrations up to 3 w%; the foamability and foam stability data are shown in Fig. 1.38. These plots indicate an initial increase in foamability up to 0.5 w% amine which remains fairly constant at higher amine concentrations, while the foam stability does not show a substantial increase until

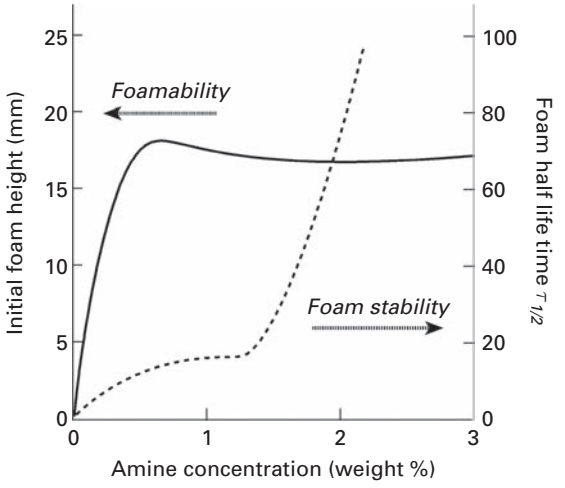

Fig. 1.38 Plot of foamability and foam stability versus amine concentration for a system of silica nanoparticles (10 w%) in n- amylamine. The foams were generated by microfluidics and the initial foam height (foamability) and the foam half-life $t_{1/2}$ (foam stability) were determined by filling vials during a fixed period of time (45 s) and by filming individual layers of bubbles for better visibility. From ref (64).

an amine concentration of about 1.5 w% is reached. In order to optimize this system to achieve a balance of high foamability with a fairly high foam stability, an amine concentration of about 2 w% could be chosen. This behavior contrasts with the handshaking foaming performance on the same amine/silica particle system in which a maximum in foam height was reported between 0.5 and 1 w% amine at 1 w% solid particles. However, it would be of interest to carry out further experiments in the different foaming regimes (by varying the particle concentration). Interestingly, extremely high foam stability was explained in these systems by gelled interfaces.

Azira and coworkers (65) showed that the isomeric molecular distribution in surfactants can also influence the foaming characteristics. In these studies both the foamability and foam stability of two samples of dodecanesuphonate as a function of their isomeric distribution (using the Ross–Miles foaming test) were compared. The highest foaming performance was obtained with samples rich in primary isomers, and these systems also gave high stability. Samples rich in secondary isomers gave a comparable foamability but the foam stability was found to be lower. This behavior is useful in designing low foaming dishwashing liquids. Generally, the best foaming performance was obtained near the CMC as anticipated.

1.12.1 Surface tension, foamability and foam stability

Although a low dynamic surface tension usually corresponds to a high foamability, foam stability is usually more dependent on the viscoelasticity and repulsive interactions within thin film lamellae. However, the situation is complex since with low foaming surfactant solutions it is difficult to obtain an absolute value of the initial foam volume or height because foam decay may occur in parallel with the foam generation step. This was illustrated in a series of experiments carried out by Tamura and coworkers (66), with a series of purified dodecyl polyoxyethylene ether surfactants represented by C_{12} $(EO)_n$, in which the EO unit varied from n = 5 to 43. In this study, using concentrations above the CMC, the Ross–Miles test was used to measure foamability (expressed by the initial foam volume) and foam decay, expressed by the residual foam height ratio ($H_r/H_i \times 100\%$, where H_r is the residual foam height after 5 mins. standing and H_i is the initial residual height). The results are shown in Fig. 1.39, and it can be seen that an increase in foamability occurs with the increase in EO units, but after reaching a maximum at n = 20, it remains fairly constant. The residual foam height ratio shows an opposite effect, with a decrease in stability with increase in EO units until it reaches about n = 40 and remains constant for longer EO units. This result indicates that the surfactants with low EO units have high foamability but low stability (high decay rate) and the initial foamability results may have been underestimated since the decay process may be occurring during foam generation. Interestingly, the surfactants with high EO units have low foamability but high stability.

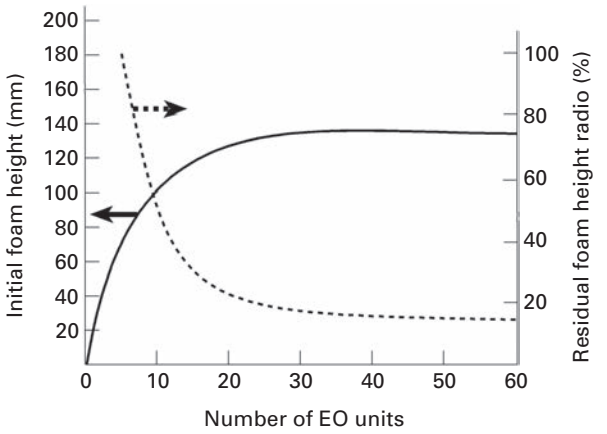

Fig. 1.39 The influence of the number of EO units on the Ross–Miles foam behavior for 1 mM $C_{12}E_n$ solution at 26° C. From ref (66).

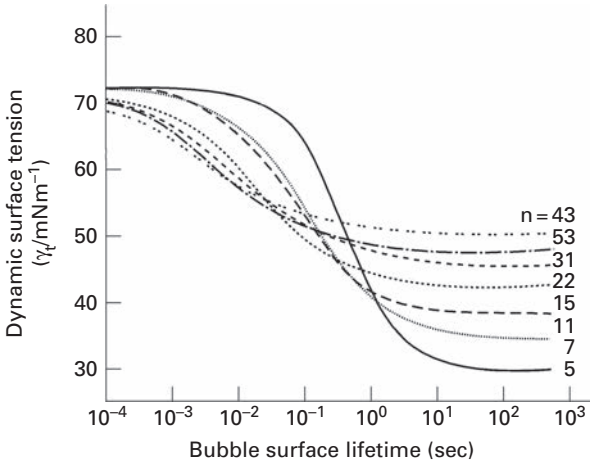

Fig. 1.40 The influence of the number of EO units on the dynamic surface tension versus bubble surface lifetime in 1 mM $C_{12}E_n$ at 26°C. From ref (66).

In addition, the dynamic surface tension of the surfactant series was determined over a range of time scales, and the results are shown in Fig. 1.40. Again, different trends in performance are indicated, with the longer chain molecules showing a fairly steep fall in surface tension at time scales from 10^{-4} to 10^{-1} seconds but leveling-off at intermediate values of surface tension, whereas the opposite effect occurred for the shorter chain molecules. This results suggests that the initial generation step corresponded to the lowest fall in surface tension with time ($d\gamma/dt$) in the region of 10^{-1} to 10^{-2} seconds suggesting a high Gibbs elasticity in this region.

1.12.2 Combining foamability with foam stability

Karakashev and coworkers (67) proposed an interesting concept, based on a new parameter which was designated "foam production" which combined foamability with foam decay. Primarily, the Bikerman test of foaminess (68), as described in Chapter 11, is expressed in units of seconds, is sensitive for low-medium foaming systems and is defined by the relationship;

$$\Sigma = \frac{H_e}{U_g} \tag{1.15}$$

where H_e is the equilibrium height of foams and U_g is the superficial gas rate. In this test the foam decay is usually estimated from an average value of the time of breakdown.

However, alternative methods of generating foam can be used such as agitation which may give short lived foams (transient) but not for more stable tenacious foams. For the transient foams, the elastic modulus of air/water interface was considered to play a major role in foaming and decay. In the case of the more stable tenacious foams (which have specific internal structure with polyhedral lamellae, Plateau borders, etc.), the breakdown process was dominated by drainage and coarsening rather than elasticity. The foam production parameter was defined as

$$F_p = \frac{\Sigma}{U_d} \tag{1.16}$$

where Σ is the Bikerman unit of foaminess while U_d is the foam decay rate. However, since this definition was only valid for the Bikerman test involving sparging gases and it was necessary to have a second definition of foam production (F_p^*), which could be applied to other generation methods such as agitation, it was expressed as

$$F_p^* = \frac{V_i}{U_d} \tag{1.17}$$

where V_i is the initial foam volume and U_d is the average rate of foam decay. Using this approach, the foam production of solutions of sodium octylsulfate and sodium decylsulfate was determined by both the Bikerman (sparging) method and shaking at fairly low concentrations (below the concentration where association of the surfactant species occurs commonly, known as the critical concentration level or CMC). The results for the Bikerman test are shown in Fig. 1.41.

From these experiments, it was found that the foam production parameter increases linearly with C/CMC up to values of 0.15–0.2 C/CMC for both surfactant systems, with the sodium decylsulfate giving higher performance. However, in the shaking method, although a linear response was obtained for both surfactants, the performance was

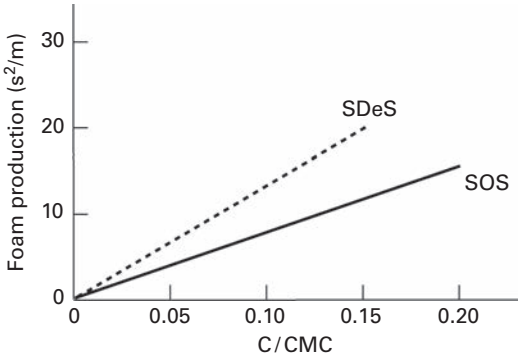

Fig. 1.41 Foam production versus C/CMC for sodium octylsulfate (SOS) and sodium decylsulfate (SDeS) versus C/CMC using the Bikermann method of foam generation (sparging of gas into the surfactant solution in a column). From ref (67).

higher for sodium octylsulfate than for sodium decylsulfate. Clearly, this concept demands further investigation.

1.13 Transition from wet to dry foams

With regard to the initial generation of the wet bubbles, the most common stabilization mechanisms occur at the molecular level and involve the Gibbs–Marangoni effect, which acts to stabilize the bubbles. The transition from bubbles to rigid foams occurs over an increasing range of time and length scales, as illustrated in Fig. 1.42. At the short end of the time and length scales (involving milliseconds and nanoscale sizes), extremely small structures are predominant. These systems have been developed as monodispersed crystalline bubble assemblies in confined channels. They have been produced by microfluidic techniques and have been shown to have interesting applications in the areas of fundamental research and industrial development such as in lab-on-chip technology (69).

Generally, wet foams are in a continuous state of evolution, and on extending the time scale, the stability is continuously reduced due to three key processes. Primarily, due to gravitation forces, drainage occurs from between the bubbles and surface viscosity, bulk viscosity and surface elasticity influence the drainage rate and stability causes a reduction in both the liquid fraction and film thickness. Secondly, coarsening occurs due to molecular gas diffusion between bubbles (disproportionation) once a critical bubble size is reached and this gives an increase in mean bubble size, ranging from tens of microns to several centimeters. This effect can be reduced by using less soluble gases. In addition, evaporation occurs when foams are exposed to the atmosphere, causing rupture of upper films. As coarsening proceeds, the foam approaches the wet limit, resulting in compaction which acts to cause cell opening and destabilization.

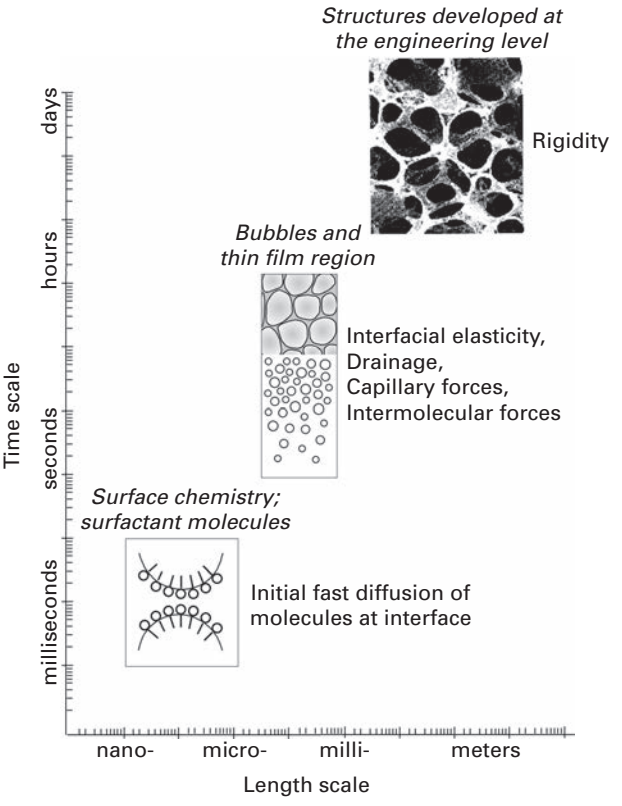

Fig. 1.42 An overview of the transition from wet to dry foam.

As the transition proceeds, films can rupture and structural rearrangement occurs. With wet closed polymer cells, faces may be formed which collapse giving an open-cell structure. Eventually, as the entire large-scale collective system evolves, it finally gels and transforms to a dry foam. Interestingly, on the large end of the length and time scale, the astrophysicists have applied huge bubbles and foam structures to describe the galactic structure of the cosmos and the fabric of scale-time. Recent models suggest that the curved space of the universe is not filled with galaxies but is mostly empty, with the galaxies lying on the surface of dodecahedral bubbles which constitute a gigantic foam (70).

References

(1) W. Wayt Gibbs and N. Myhrvold, The Incredible Edible Foam, *Scientific American*, p. 10, December 2010.
(2) The Science Physics of Exotic Soap Bubbles, *The Daily Telegraph*, November 24, 2007.

(3) R. J. Pugh, *Foam Breaking in Aqueous Solution, Handbook of Applied Surface and Colloid Chemistry*, Ed. K. Holmberg, Chapter 8, pp. 143–157, John Wiley and Sons, 2002.
(4) S. Lu, R. J. Pugh and E. Forssberg, *Interfacial Separation of Particles, Studies in Interface Science*, **20**, Elsevier Publications, 2005.
(5) N. Barbian, K. Hadler, E. Ventura-Medina and J. J. Cilliers, The Froth Stability Column Linking Froth Stability and Flotation Performance, *Min. Eng.*, **18**, 317–324, 2005.
(6) K. Theander and R. J. Pugh, Surface Chemical Aspects of Flotation Deinking, *Colloid Surf. A*, **240**, 111–130, 2004.
(7) L. L. Schramm, Foams: Fundamentals and Applications in the Petroleum Industry (Advances in Chemistry Series), *Am. Chem. Soc*., **242**, 1994.
(8) N. J. Mills, *Running Shoe Case Study, Polymer Foam Handbook*, Elsevier Publications, Chapter 13, p. 308, 2005.
(9) Foam that Stems Troops' Wounds, *Daily Mail*, Tuesday, p. 26, June 18, 2013.
(10) C. S. Pereira, M. E. Gomes, R. L. Reis and A. M. Cunha, Hard Cellular Materials in the Human Body. Properties and Production of Foamed Polymers for Bone Replacement. In *Foams and Emulsions*, Ed. J. F. Sadoc and N. Rivier, Kluwer Academic, pp. 193–206, 1999.
(11) D. W. Thomas, *On Growth and Form*, 2nd edn, Cambridge University Press, 1942.
(12) C. S. Smith, *A Search for Structure, Selected Essays in Science, Art and History*, MIT Press, Cambridge, Mass., 1981.
(13) D. Weaire and S. Hutzler, *The Physics of Foams*, Clarendon Press, Oxford, 1999.
(14) W. Drenckhan and A. Saint-Jalmes, The Science of Foaming, Historical Perspective, *Adv. Colloid Interface Sci.*, **222**, 228–259, 2015.
(15) K. A. Brakke, The Surface Evolver, *Exp. Maths*, **1**, 141–165, 1992, www.susqu .edu/brakke/evolver/.
(16) A. M. Kraynik, D. A. Reinelt and F. van Swol, Structure of Random Foams, *Phys. Rev. Lett.*, **93** (20), 20830-1–208301-4, 2004.
(17) J. A. F. Plateau, *Statique Experimentale et Theorique des Liquids Soumis aux Seules Forces Moleculaires*, **2**, Clemm, Belgium. 1873.
(18) C. L. Strong, How to Blow Soap Bubbles That Last for Months or Even Years, *Sci. Am.*, **220** (5), 128–132, 1969.
(19) M. Vignes-Adler and D. Weair, New Foams: Fresh Challenges and Opportunities *Curr. Opin. Colloid Interface Sci.*, **13**, 141–149, 2008.
(20) R. J. Pugh, Foaming, Foam Films, Antifoaming and Defoaming, *Adv. Colloid Interface Sci.*, **64**, 67–142, 1996.
(21) J. J. Bikermann, *Foams*, Springer-Verlag, New York, 1973.
(22) J. A. Kitchener and C. F. Cooper, Current Concepts in the Theory of Foaming, *Q. Rev., Chem. Soc.*, **13**, 71–79, 1959.
(23) T. Young, An Essay on the Cohesion of Fluids, *Philos. Trans. R. Soc. London*, **95**, 65, 1805.
(24) J. A. F. Plateau, *Statique Experimentale et Theorique des Liquides Soumis aux Seules Forces Moleculaires*, Gauthier-Villars, Paris, 1873.
(25) W. Thompson (Lord Kelvin), On the Division of Space with Minimum Partitional Area, *Acta Math.*, **11**, 121–134, 1887.

(26) A. M. Kraynick and W. E. Warren, *The Elastic Behavior of Low-Density Cellular Plastics, Low Density Cellular Plastics*, Ed. N. C. Hilyard and Coworkers, Chapman and Hall, 1994.
(27) D. Weaire and R. Phelan, A Counter-Example to Kelvins Conjecture on Minimal Surfaces, *Phil. Mag. Lett.*, **69**, 107–110, 1994.
(28) H. Fountain, A Problem of Bubbles Frames an Olympic Design, *New York Times*, August 5, 2008, www.nytimes.com/2008/08/05/sports/olympics/05swim.html.
(29) R. Gabbrielli, A. J. Meagher, D. Weaire, K. A. Brakke and S. Hutzler, An Experimental Realization of the Weaire-Phelan Structure in Monodispersed Liquid Foam, *Philos. Mag. Lett.*, **92** (1), 1–6, 2012.
(30) R. E. Williams, Space Filling Polyhedron: Its Relation to Aggregates of Soap Bubbles, Plant Cells and Metal Crystallites, *Science*, **161**, 276–277, 1968.
(31) A. W. Adamson and A. D. Gast, *Physical Chemistry of Surfaces*, 6th edn, John Wiley and Sons, 1997.
(32) E. B. Matzke, The Three Dimensional Shape of Bubbles in Foam – Analysis of the Role of Surface Forces in Three Dimensional Cell Shape Determination, *Am. J. Bot.*, **33** (1), 58–80, 1946.
(33) T. Szekrenyesy, K. Liktor and N. Sador, Characterization of Foam Stability by the Use of Foam Models, Part 1 Models and Derived Lifetimes, *Colloid Surf.*, **68**, 267–273, 1992 and Part 2, Results and Discussion, *Colloid Surf.*, **68**, 275–282, 1992.
(34) L. Bragg and J. F. Nye, A Dynamic Model of a Crystal Structure, *Proc. Royal Soc., London*, **A190**, 474–481, 1947.
(35) C. S. Smith, On Blowing Bubbles for Braggs Dynamics Crystal, *J. Appl. Phys.*, **20**, 631, 1949.
(36) M. Arciniaga, C. Kuo and M. Dennin, Size Dependent Brittle to Ductile Transitions in Bubble Rafts, *Colloids Surf., A*, **382**, 36–41, 2011.
(37) A. van der Net, W. Drenckham, D. Weaire and S. Hutzler, The Crystal Structure of Bubbles in the Wet Foam State, *Soft Matter*, **2**, 129–134, 2006.
(38) A. J. Meager, D. McAteer, S. Hutzler and D. Weaire, Building the Pyramids; Perfect Bubble Crystals, *Phil. Mag.*, **93**, 31–33, 2013.
(39) S. T. Tobin, J. D. Barry, A. J. Meagher, C. E. O'Rathaille and S. Hutzler, Ordered Polyhedral Foams in Tubes with Circular, Triangular and Square Cross Section, *Colloids Surf., A*, **322**, 24–31, 2011.
(40) N. D. Denkov and K. G. Marinova, Antifoam Effects of Solid Particles, Oil Droplets and Oil Solid Compounds in Aqueous Foams. In *Colloidal Particles at Liquid Interfaces*, Ed. B. P. Binks and T. Horozov, Chapter 10, Cambridge University Press, Cambridge, 2006.
(41) Y. You, X. Wu, J. Zhoa, Y. Ye and W. Zou, Effect of Alkyl Tail Length of Quaternary Ammonium Gemini Surfactants on Foaming Properties, *Colloids Surf., A*, **384**, 164–171, 2011.
(42) P. Ball, Water: Water – An Enduring Mystery, *Nature*, **452**, 291–292, 2008.
(43) F. Franks, *Water: A Comprehensive Treatise*, Vol. **1**, Plenum Press, NewYork, 1975.
(44) L. G. M. Pettersson and Coworkers, Diffraction and IR/Raman Data Do Not Prove Tetrahedral Water, *J. Chem. Phys.*, **129** (8), 2008.
(45) K. Lunkenheimer, *Surface-Chemical Purity of Surfactants: Phenomena, Analysis, Results, and Consequences. Encyclopedia of Surface and Colloid Science*, 2nd edn, Taylor and Francis, NewYork, pp. 5879–5906, 2006.

(46) C. Stubenrauch and K. Khristov, Foam and Foam Films Stabilized by Influence of Chain Length and Impurities, *J. Colloid Interface Sci.*, **286**, 710–718, 2005.
(47) A. C. Newell and B. Rumpf, Wave Turbulence, *Ann. Rev. Fluid Mech.*, **43**, 59–78, 2011.
(48) G. B. Deane and M. D. Stokes, Scale Dependence of Bubble Creation Mechanisms in Breaking Waves, *Nature*, **418**, 839–844, August 22, 2002.
(49) *Sea Foam Blizzard in England*. Courtesy of Jason Samenow, Weather Editor, The Washington Post, DC, December 30, 2011.
(50) J. W. Gibbs, *Collected Works*, Vol. **1**, Longmans Green, NewYork, 1931.
(51) F. M. Menger and S. A. A. Rizvi, Relationship between Surface Tension and Coverage, *Langmuir*, **27**, 13975–13977, 2011.
(52) V. Bergeron, Disjoining Pressure and Film Stability of Alkylmethylammonium Bromide Foam Films, *Langmuir*, **13** (13), 3474–3482, 1997.
(53) C. G. M. Marangoni, On the Principle of Surface Viscosity of Liquids by Mr. J. Plateau, Il Nuovo Cimento, Ser. **2** (5), 1872.
(54) H. Christenson and V. V. Yaminsky, Soluble Effects of Bubble Coalescence, *J. Phys. Chem.*, **99** (25), 10420, 1995.
(55) A. Prins, Surface Rheology and Practical Behaviour of Foams and Thin Liquid Films, *Chem. Ing. Tech*., **64** (1), 73, 1992.
(56) S. S. Dukhin, G. Kretzschmar and R. Miller, *Dynamics of Adsorption at Liquid Interfaces, Studies in Interfacial Science Series*, Vol. **1**, Elsevier Publications, 1995.
(57) S. Um, E. Poptoshev and R. J. Pugh, Aqueous Solutions of Ethyl (Hydroxyl Ethyl) Cellulose and Hydrophobic Modified Ethyl (Hydroxyl Ethyl) Cellulose Polymer; Dynamic Surface Tension Measurements, *J. Colloid Interface Sci*., **193**, (1), 41–49, 1997.
(58) A. Prins, The Stagnant Surface Behavior and its Effect on Foam and Film Stability, *Colloids Surf., A*, **149**, 467–473, 1999.
(59) A. Prins and D. J. M. Bergink-Martens, *Dynamic Surface Props in relation to the Dispersion Stability and Mechanical Properties, Food Colloids and Polymer stability*, Ed. E. Dickinson and P. Walstra, Cambridge, 1993.
(60) L. Rayleigh, *Foams in Scientific Papers by Lord Rayleigh*, Cambridge University Press, 1902.
(61) E. A. Howell, C. M. Megaridis and Mc Nallan, Dynamic Surface Tension Measurements of Molten Sn/Pb solder Using Oscillating Slender Elliptical Jets, *Int. J. Heat Fluid Flow*, **25**, 91–102, 2004.
(62) J. Ross and G. D. Miles, An Apparatus for Comparison of Foaming Properties of Soaps and Detergents, *Oil and Soap*, **18**, 99–102, May 1942.
(63) *Personal Communication*, Ed. M. Anderson, YKI, Institute for Surface Chemistry, Stockholm, Sweden, 2009.
(64) L. R. Arriaga and Coworkers, On the Long-term Stability of Foams Stabilised by Mixtures of Nano-particles and Oppositely Charged Short Chain Surfactants, *Soft Matter*, **43**, 11085–11097, 2012.
(65) H. Azira, A. Tazerouti and J. P. Canselier, Study of Foaming Properties and Effect of the Isomeric Distribution of Some Anionic Surfactants, *J. Surfactants Deterg.*, **11**, 279–286, 2008.

(66) T. Tamura, Y. Kaneko and M. Ohyama, Dynamic Surface Tension and Foaming Properties of Aqueous Polyoxyethylene n-Dodecyl Ether Solutions, *J. Colloid Interface Sci.*, **173**, 493–499, 1995.
(67) S. Karakashev, P. Georgiev and K. Balashev, Foam Production – Ratio between Foaminess and Rate of Foam Decay, *J. Colloid Interface Sci.*, **379**, 144–147, 2012.
(68) J. J. Bikerman, Measurements of Foaminess, Chapter 3, *Foams*, Springer-Verlag, Berlin, 1973.
(69) D. Weaire and W. Drenckhan, Structure and Dynamics of Confined Foams; A Recent Progress Report, *Adv. Colloid Interface Sci.*, **137** (1), 20–26, 2008.
(70a) A. Fairall, *Large Scale Structures in the Universe*, Wiley, Chichester, 1998; (b) J. A. Wheeler, Geons, Black Holes and Quantum Foams, *A Lifetime in Physics*, 2000.